ANL-5276

-1-

ARGONNE NATIONAL LABORATORY
P. O. Box 299
Lemont, Illinois

HEAT TRANSFER TO BOILING WATER FORCED THROUGH A UNIFORMLY HEATED TUBE

by

J. F. Mumm*

Reactor Engineering Division

November, 1954

This report is based on a thesis submitted in partial fulfillment of the requirements for the Degree Master of Science in Mechanical Engineering in the Graduate School of the Illinois Institute of Technology.

* Present Address: Babcock and Wilcox Co. Akron, Ohio

Operated by The University of Chicago
under
Contract W-31-109-eng-38

DISCLAIMER

DISCLAIMER

2

TABLE OF CONTENTS

3

LIST OF FIGURES

NOMENCLATURE

Symbol	Definition	Units
A	Area	sq ft
B	Orifice coefficient	
C_n	Constant, n = 1, 2, 3	
c_p	Specific heat at constant pressure	Btu/lb
D	Inside diameter of tube	ft
D_e	Equivalent diameter of system	ft
D_b	Bubble diameter	ft
f	Frequency	
G	Mass flow rate per unit area	lb/(hr)(sq ft)*
g	Functional relationship	
h_c	Coefficient of heat transfer utilizing the temperature between the wall and the bulk fluid = $8''/\theta_c$	Btu/(hr)sq ft) (F)
h_{fg}	Latent heat of vaporization	Btu/lb
h	Coefficient of heat transfer utilizing the temperature difference between wall and saturation temperature which may or may not be the temperature of the bulk fluid	Btu/(hr)(sq ft)(F)
h_{sc}	Scale coefficient of heat transfer	Btu/(hr)(sq ft)(F)
k	Thermal conductivity	Btu/(hr)(ft)(F)
L	Length	ft
m	Mass flow rate	lb/hr
N_B	Dimensionless group, $\frac{q''}{Gh_{fg}}$	
N_{Nu}	Nusselt Number, $\frac{hD_e}{k}$	
N_{Pr}	Prandtl Number, $\frac{\mu c_p}{k}$	
N_{Re}	Reynolds' Number $\frac{G\,D_e}{\mu}$	
p_r	Reduced Pressure	

* Unless otherwise defined

NOMENCLATURE (Cont'd.)

Symbol	Definition	Units
q	Total heat transferred per unit time	Btu/hr
q''	Heat flux	Btu/(hr)(sq ft)
r_1	Inside radius	ft
r_2	Outside radius	ft
s	Thickness	ft
t	Temperature	F
U	Over-all coefficient of heat transfer	
V	Specific volume	cu ft/lb
x	Fraction of flow evaporated	
β	Ratio, orifice diameter to pipe diameter	
γ	Specific weight	lb/cu ft
θ_{sat}	$t_w - t_{sat}$	F
θ_c	$t_w - t_b$	F
θ	Temperature excess	F
μ	Viscosity	lb/hr

Subscripts

b	Bulk stream
f	Liquid
fg	Denotes change in property from liquid phase to vapor phase
g	Vapor
sat	Saturation
w	Wall

6

HEAT TRANSFER TO BOILING WATER FORCED THROUGH A UNIFORMLY HEATED TUBE

by

J. F. Mumm

ABSTRACT

An electrically heated, horizontal, Type 347 stainless steel tube (0.465 in. ID by 0.505 in. OD by 7 ft long) was used to obtain local coefficients of heat transfer in the region of net steam generation. The maximum weight fraction evaporated was 0.60. The investigation covered a range of pressures from 45 to 200 psia, of heat fluxes from 50,000 to 250,000 Btu/(hr)(sq ft), and of flow rates from 70 to 280 lb/(sec) (sq ft).

The data were correlated by means of the dimensionless equation

$$\frac{h\,D_e}{k} = \left[4.3 + 5.0 \times 10^{-4} \left(\frac{V_{fg}}{V_f}\right)^{1.64} x\right] \left[\frac{q''}{Gh_{fg}}\right]^{0.464} \left[\frac{GD_e}{\mu_f}\right]^{0.808}$$

with a root mean square deviation of 10%.

I. INTRODUCTION

Recent technological advances have focused an ever increasing amount of attention on the boiling phenomenon as a means of increasing the magnitude of the heat removed per unit area. The purpose of this investigation was to measure the rate of heat transfer to steam-water mixtures during forced flow through a uniformly heated channel and to examine the effect of quality, heat flux, flow rate, and absolute pressure on this rate.

The scope of the work reported is limited to forced circulation of water through a horizontal round tube with the following approximate range of variables:

(1) Mass velocity: 70 to 280 lb/(sec)(sq ft). This corresponds to inlet liquid velocities of 1.5 to 6 fps.
(2) Absolute pressure: 45 to 200 psia.
(3) Heat flux: 50,000 to 250,000 Btu/(hr)(sq ft). This corresponds to a maximum power input of 53 kw to the test section.
(4) Fraction of flow evaporated: 60% maximum.

II. LITERATURE SURVEY

There is rather extensive literature available which pertains to boiling. An excellent review of the subject is given in a paper by Rohsenow(1) who presents the salient features of more than 50 investigations.

An extremely small amount of work has been done in the area of investigation covered by the author. Stroebe, et al.,(2) boiled water, sugar, and "Duponal" solutions in a 20-foot long vertical evaporator. Average individual coefficients were obtained for the entire tube. The results were correlated empirically in terms of the Prandtl Number, surface tension of the liquid, specific volume of the vapor, and the average temperature drop from the tube wall to the bulk stream, all of this based on the average temperature of the boiling liquid. The fact that the variation of the difference between wall and bulk temperature from one end of the tube to the other was large compared to the range of the mean values of this difference makes the correlation of little value for determining point coefficients. It was observed, however, that the heat transfer coefficients decreased after 50% vaporization of the fluid.

Davidson, et al.,(3) investigated heat transfer and pressure drop in flat helical coils exposed on one side to furnace heat. They succeeded to some degree in using the magnitude of the dimensionless parameter $\frac{q''}{G\, h_{fg}}$ as an indication for overheat conditions.

McAdams, Woods, et al.,(4) vaporized water, benzene and benzene-oil mixtures in steam-jacketed horizontal tubes. Up to 99% of the feed was vaporized during runs with boiling water. Inlet velocities ranged from 0.27 to 0.85 fps and the absolute pressure ranged from 1 to less than 2 atmospheres. Over-all coefficients of heat transfer were obtained but no correlation is cited.

The above papers constitute the bulk of the investigations of boiling with net steam generation in a dynamic system.

Earlier investigations shed some light on the mechanism of boiling. Nukiyama(5) and Farber and Scorah(6) used a platinum wire in a pool of water. The latter investigators defined the various regions of boiling. Jakob and co-workers(7) made extensive studies of bubble formation, growth and/or collapse. These investigations showed that bubble formation is preferential, i.e., bubbles form where there is a small radius available, and, therefore, depend to some extent on surface roughness. They also showed that the number of originating points depends on the heat flux.

There are no general correlations available in the literature that pertain to the area of investigation covered in this report.

III. EXPERIMENTAL APPARATUS

A. General Description

The apparatus described is the same as that used by George Leppert[8] for pressure drop measurements. Certain aspects of the design are the result of joint effort; these include the method of recirculation of the water and the maintenance of water purity. The instrumentation for obtaining temperature measurements are primarily the author's responsibility.

Figure 1 shows a pictorial representation of the major components of the test apparatus, which consists of a closed loop which is filled with distilled water. Water flows from the bottom of the supply tank to the first-stage, turbine-type centrifugal pump and then to the second-stage pump. The pump bodies were iron, the impellers, bronze. A turbine-type pump (Aurora Pump Co., Model D5T) was chosen because of its steep head-discharge curve, which offers the advantage that a large increase in pressure drop causes a relatively small decrease in flow. Figure 2 shows the pump characteristics for the motor speeds of 1150 and 1750 rpm used in the experiment.

The pump discharged into parallel orifice assemblies which were fitted with gate valves so that the flow could be directed through either of two calibrated orifices. These orifices were machined and assembled in 1-inch pipe in the manner described by Grace and Lapple,[9] except that the thin-plate orifices were machined with edges 0.005 in. or less instead of the 0.001 in. or less for the knife edge orifices used by those authors. It is believed that the duller edges account for the slightly lower orifice coefficients obtained by weigh-tank calibration (Figs. 3 and 4), as compared to the Grace and Lapple[9] coefficients.

Figure 5 is a schematic diagram of the orifice pressure tap connections. Either orifice may be connected to the differential-pressure transmitter (Brown Model No. 228N5G2) and to the U-tube manometer which is in parallel with the transmitter. The manometer was used for flow measurement because of its accuracy, while the transmitter was used in the air-operated flow control system, shown schematically in the figure. The 3- to 15-psi air signal from the transmitter, together with the 3- to 15-psi control point air pressure, was balanced by the flow controller (Moore Nullmatic Controller Model 50F), which sent a 0- to 15-psi signal to the air-actuated throttle valve (Conoflow Model AB-10, 1/2-inch valve with interchangeable 1/4-inch and 3/8-inch ports).

Immediately after passing through the flow throttle valve, the water entered the 40-kw, 440-volt, 3-phase Calrod immersion preheater. Power to the three phases was controlled manually by means of continuously variable transformers (Powerstat Type 1256).

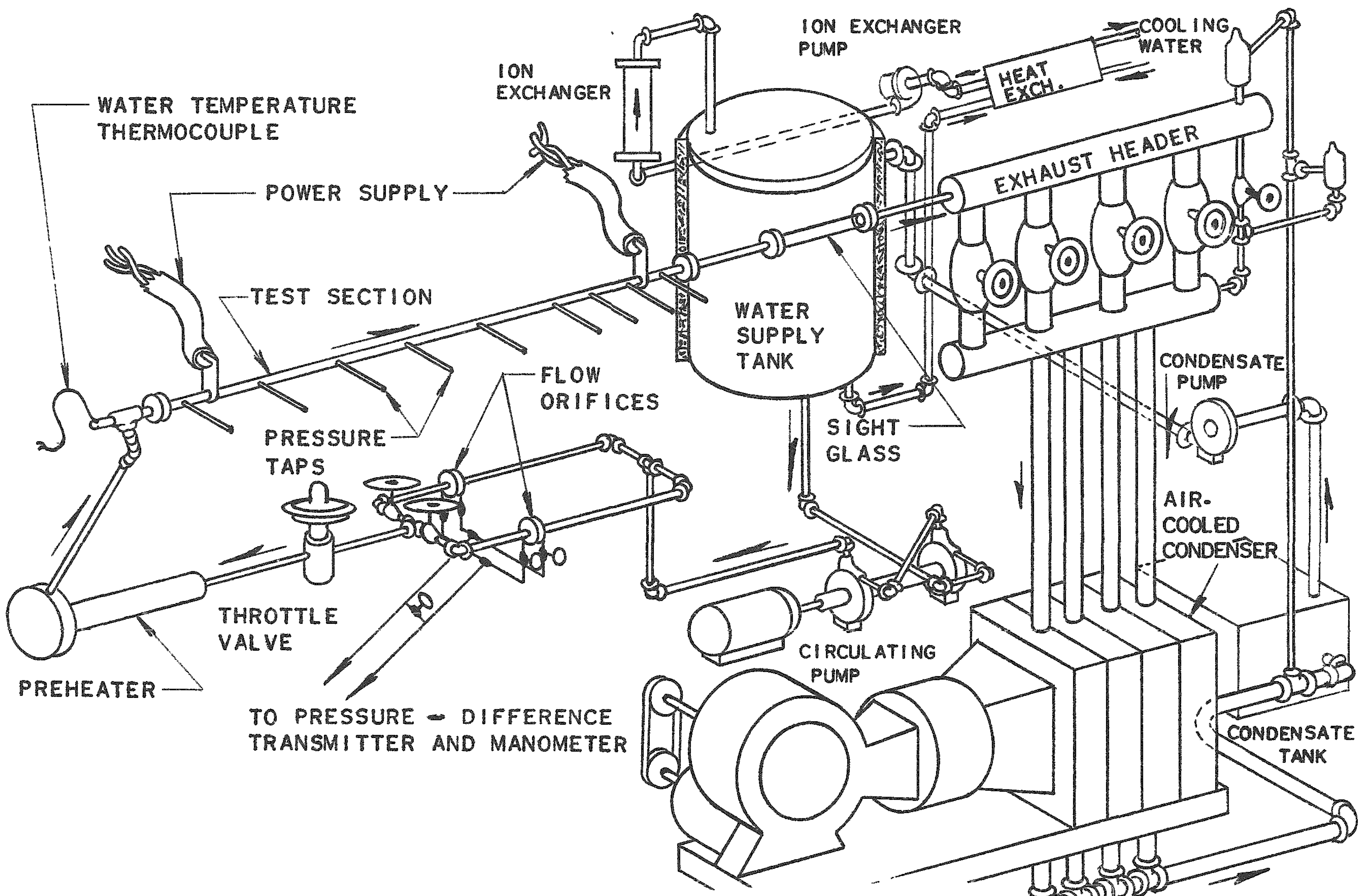

FIGURE 1 MAIN COMPONENTS OF TEST APPARATUS

10

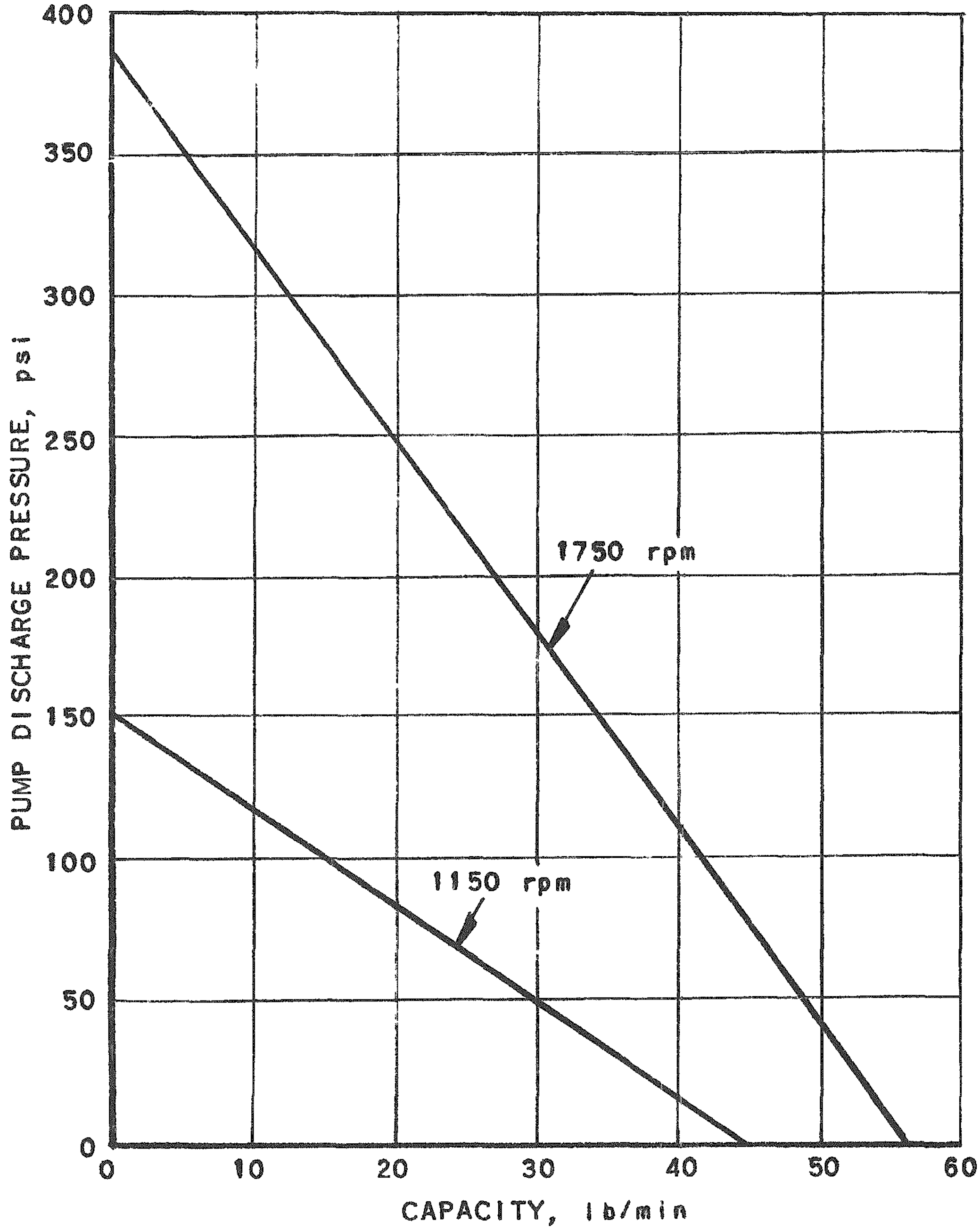

FIGURE 2 CHARACTERISTIC CURVES FOR AURORA TURBINE-TYPE PUMP, MODEL D5T

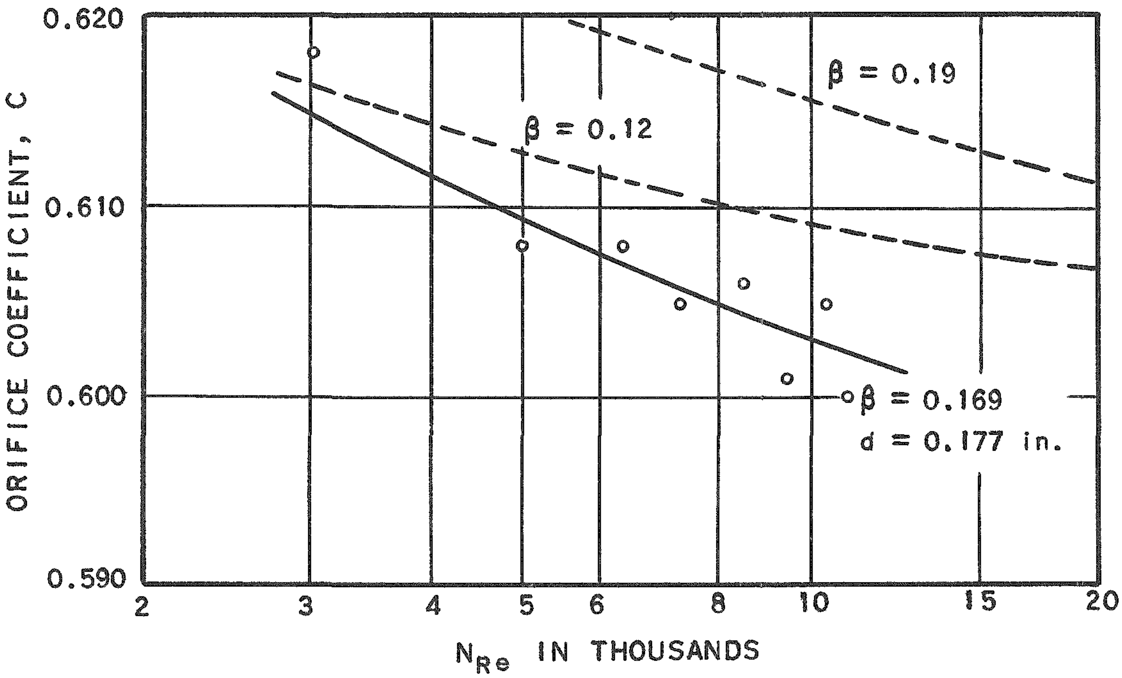

NOTE: DASHED LINES FROM REFERENCE 9

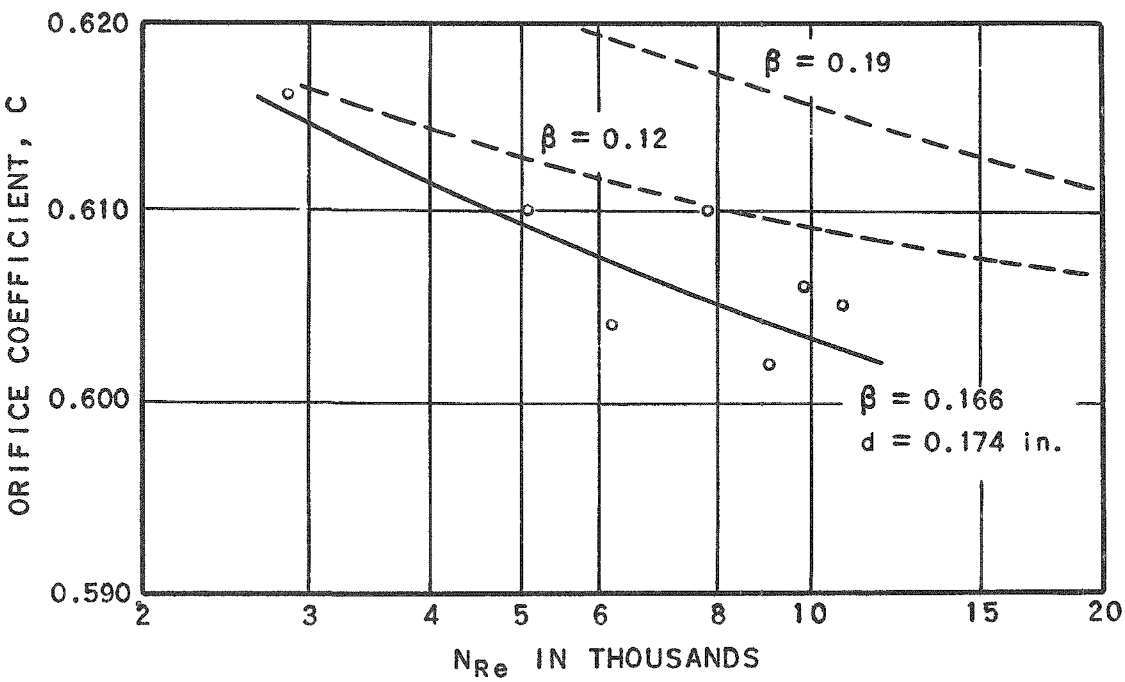

FIGURE 3 CALIBRATION CURVES FOR 0.174- AND 0.177-INCH ORIFICES

1.2

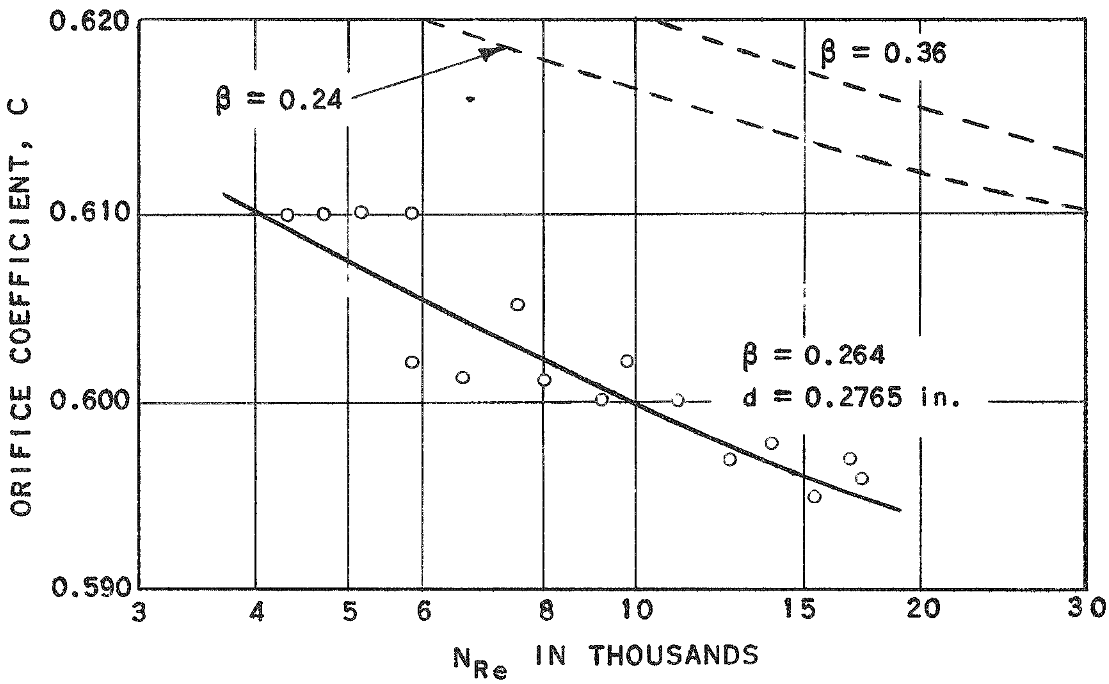

NOTE: DASHED LINES FROM REFERENCE 9

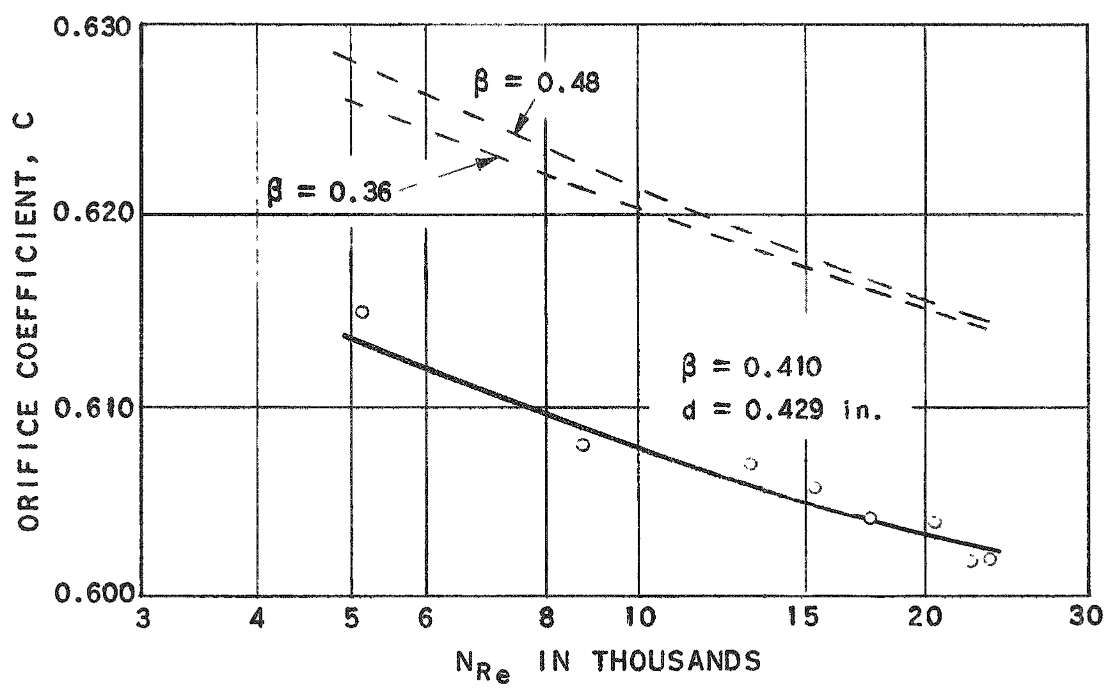

FIGURE 4. CALIBRATION CURVES FOR 0.2765- AND 0.429-INCH ORIFICES

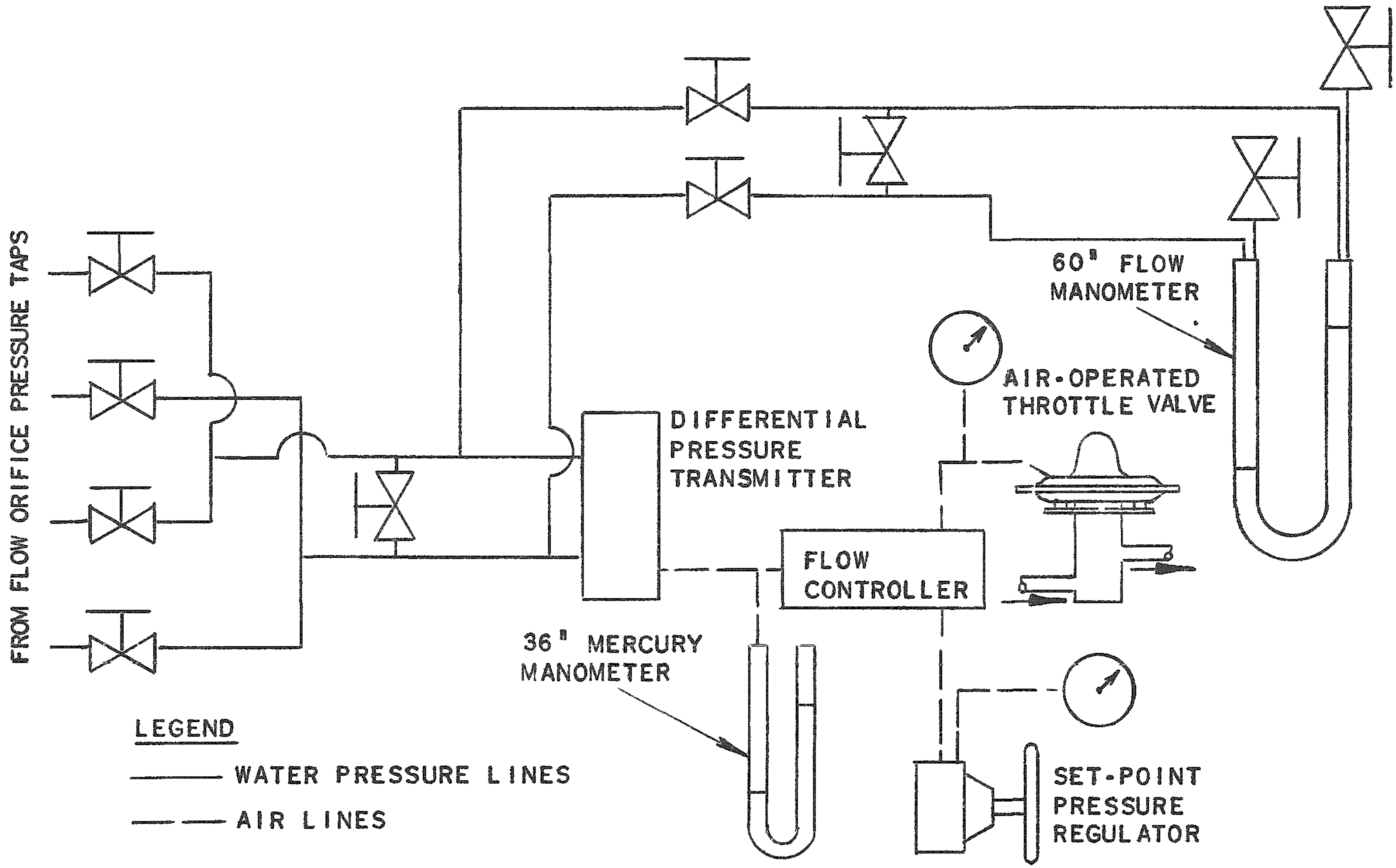

FIGURE 5 FLOW MEASUREMENT AND CONTROL SYSTEM

The water, near saturation temperature, entered the unheated portion of the test section through a pair of Teflon-insulated flanges. The temperature and pressure of the water were measured at the inlet by the use of a No. 30 iron-constantan thermocouple placed inside a copper tube, 1/8 in. OD by 1/16 in. ID, whose end was silver-soldered shut and which was immersed in the flowing water for a distance of 4-1/2 in. The inlet pressure measurement was made with a Bourdon-tube gage connected to the first pressure tap on the test section.

Electric power was brought to the test section through copper lugs silver-soldered to the surface. The alternating current was supplied by three welding transformers (Lincoln Fleet-arc 500 Industrial-Type Welder) connected in parallel. These transformers are each rated at 500 amperes at 40 volts on a 60% duty cycle with 70 volts on open circuit. The current variation was provided by a motor drive through chains and sprockets so that the transformers shared the load equally at the various settings.

The temperature of the steam-water mixture at the outlet of the test section was measured in the same manner.

The mixture passed through a sight glass (1/2 in. ID) which permitted visual examination of the flow as it left the test section.

The exhaust header was made of 4-inch Schedule 80 pipe. The four 2-inch gate valves and the single 1-inch Globe valve in parallel after the exhaust header were used to build up back pressure to the desired amount. Finally, an air-cooled condenser was provided to condense the steam before it entered the drain line to the condensate tank. A float control in this tank intermittently operated the condensate pump which returned the water to the supply tank.

All pipe and fittings after the main pump and up to and including the exhaust valves were of Type 18-8 stainless steel with the exception of the brass fittings on the test section pressure taps. Because the condenser and condensate pump were carbon steel, however, and because galvanized pipe was used in part of the condensate piping, a small ion exchanger was used to maintain the purity of the water in the system. A separate pump was used to draw water from the supply tank for purifying and subsequent return to the tank.

Figures 6, 7, and 8 are pictorial views of the experimental apparatus. Figure 8 shows the exit thermocouple connection followed by a pressure tap. The thermocouple is centrally located in the tube at the interface between flanges.

15

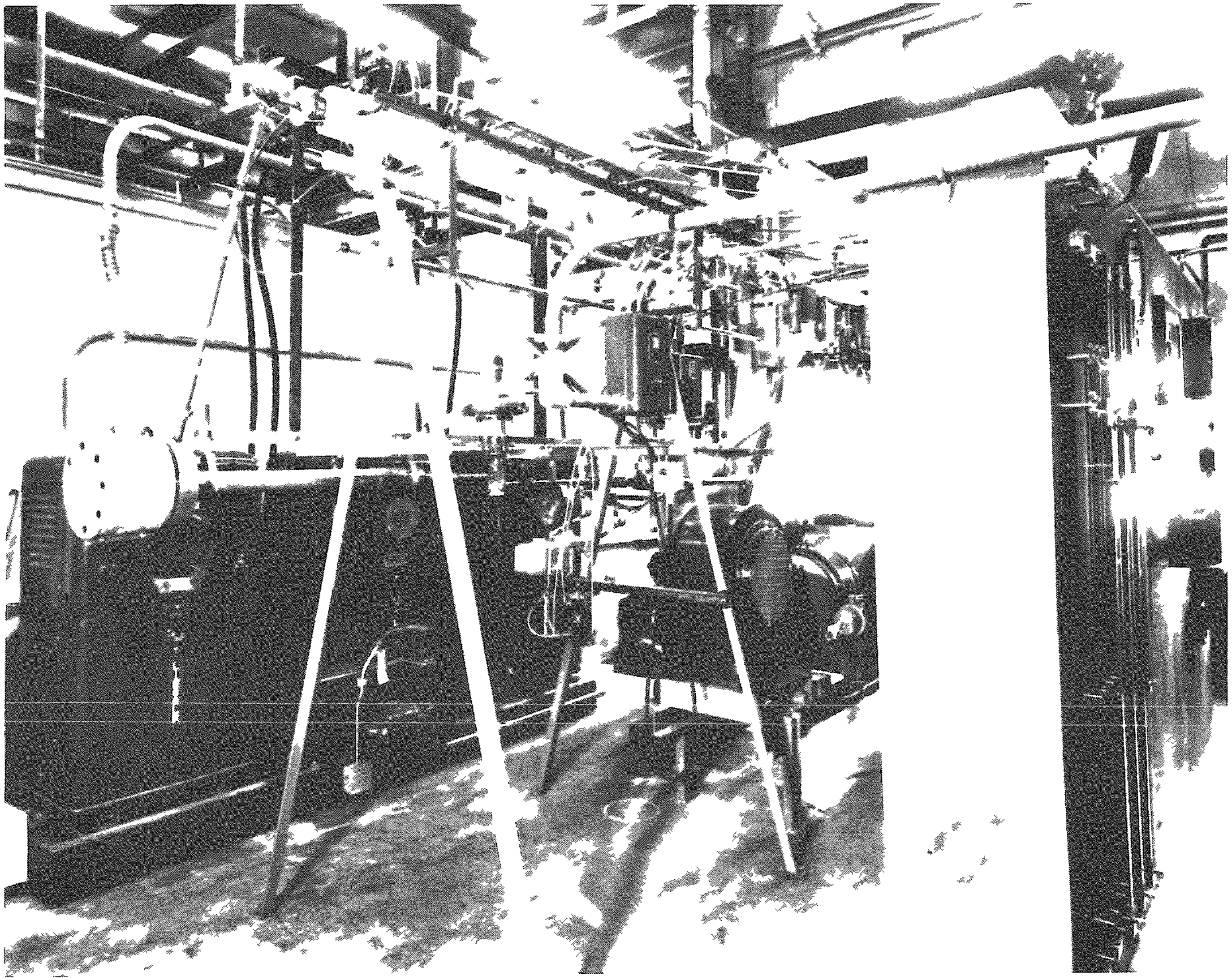

FIGURE 6 VIEW OF EQUIPMENT FROM END OF CONTROL PANEL

11.

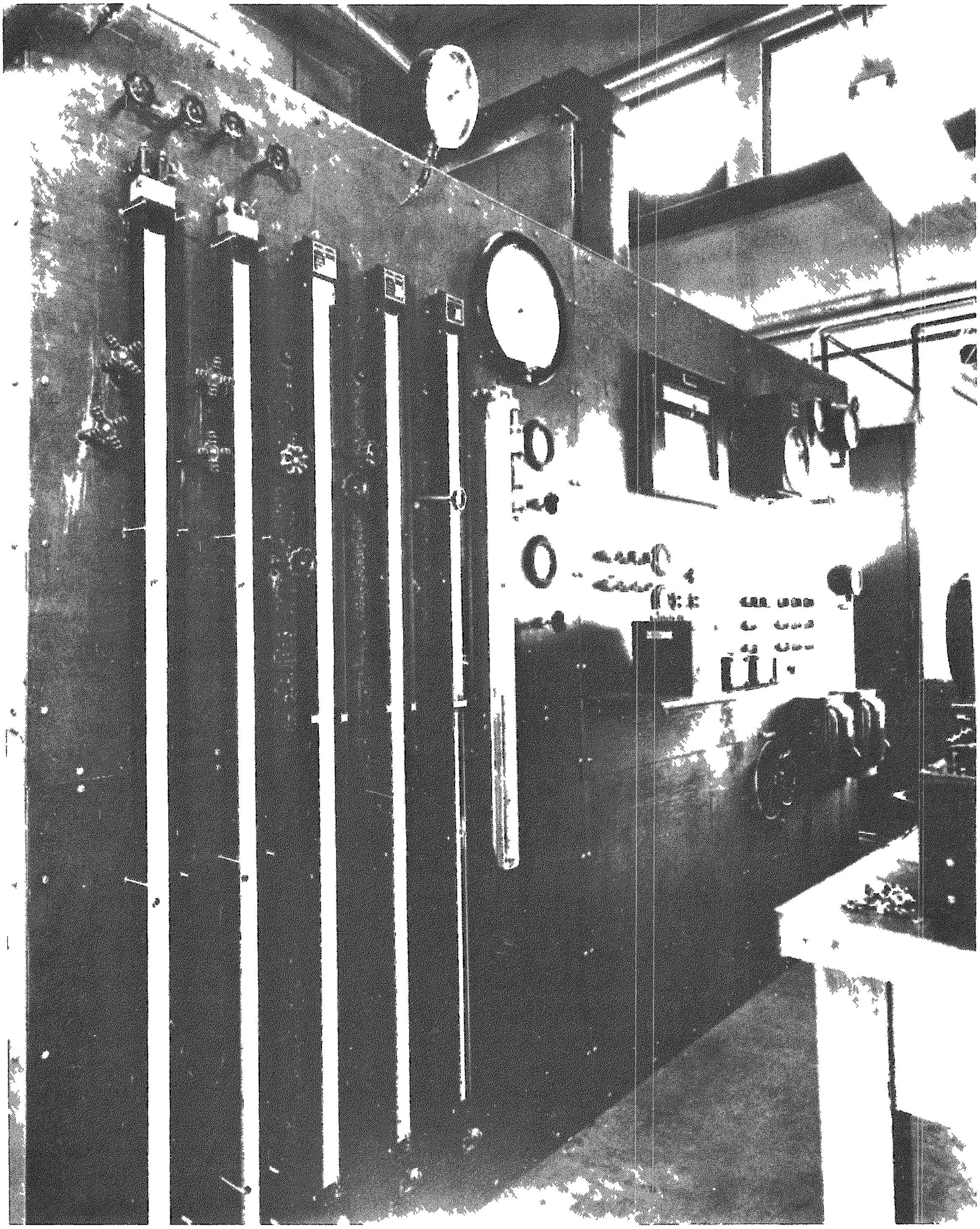

FIGURE 7 CONTROL PANEL

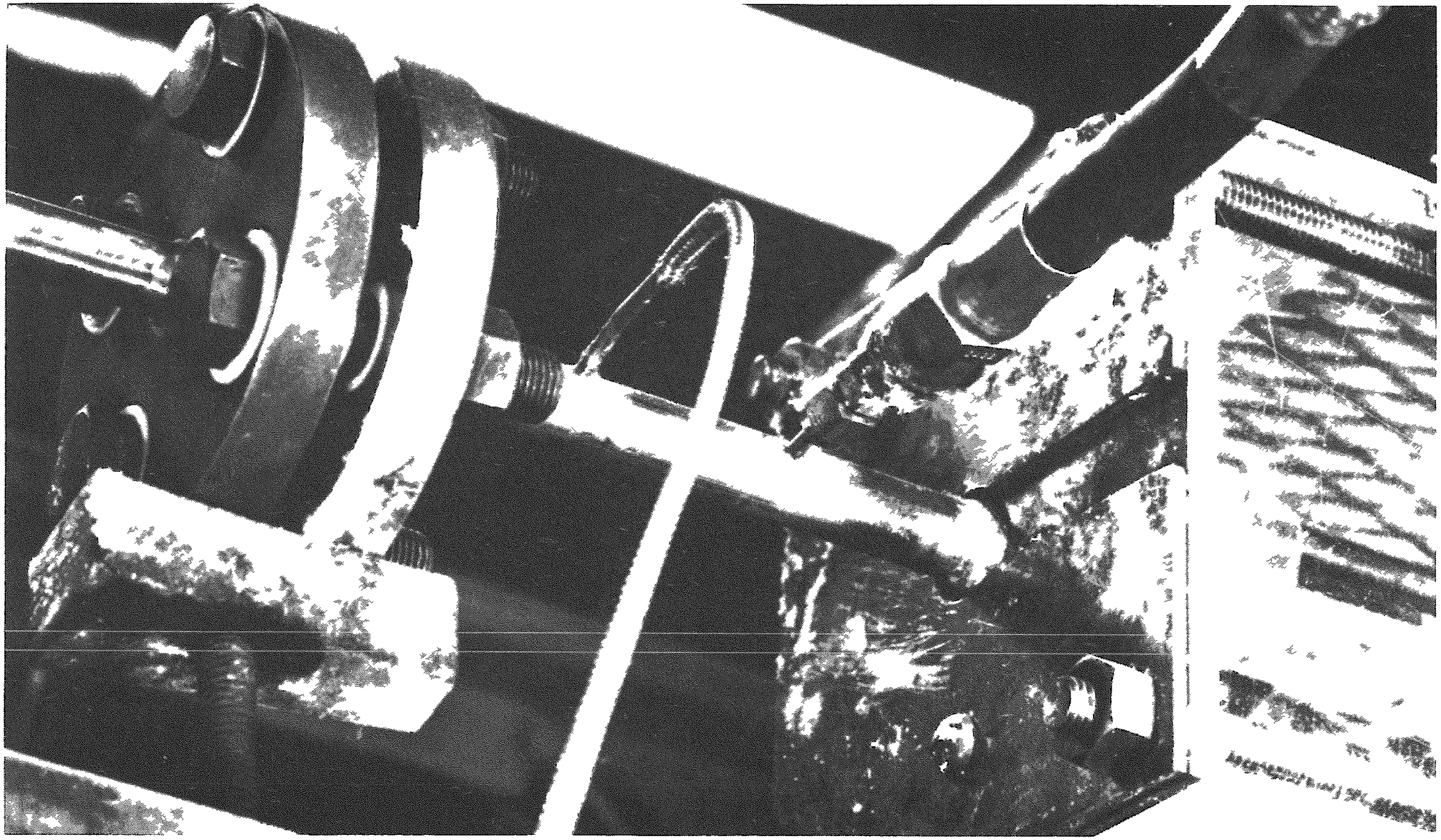

FIGURE 8 EXIT THERMOCOUPLE INSTALLATION

B. Test Section

The test section (Fig. 9) was a Type 347 stainless steel drawn tube (0.505 in. OD by 0.465 in. ID by 7 ft long). A flange was welded to each end and Teflon ring-joint gaskets were machined for each flanged connection. The flange bolts were also fitted with Teflon sleeves and washers to isolate (electrically) the test section from the remainder of the piping and framework which was grounded. The 3/8-in. thick copper lugs were silver-soldered to the test section at a distance of 6 ft between their inner faces.

The pressure taps were formed by drilling 1/32-inch radial holes through the tube wall, then running emery cloth through the tube to remove the burr in the path of the flow. A stainless tube (1/8 in. OD by 1/16 in. ID) was silver-soldered to the test section, care being taken to prevent the entry of solder or flux into the small pressure tap. After all of these small tubes had been soldered on, a final pass was made through the test section with emery cloth. A sample of a pressure tap made in this manner was cut apart for inspection; Fig. 10 shows this sample tap which, when viewed with a magnifying glass, appears to have square edges with no burr.

Forty-eight thermocouples of No. 30 iron-constantan thermocouple wire were attached to the outside surface of the test section to measure the outside wall temperature. The thermocouples were spaced at one and one-half inch intervals along the entire heated length, except that the first and last thermocouples were one-quarter inch from the copper lugs, and, therefore, only one and one-quarter inches from the adjacent couples. Each thermocouple was held to the outside surface of the tube by high-temperature glass electrical tape (Scotch Electrical Tape No. 27). Each thermocouple was wrapped around the tube approximately one-quarter turn under the glass before it is led out through the heat insulation in order to avoid error from axial conduction along the wires. Figure 11 shows a sample thermocouple installation.

To check on the uniformity of heat generation in the test section, voltage taps were attached by wrapping one turn of copper wire around the test section at distances of 5-1/2, 22, 37, 50, and 65-1/2 in. from the face of the copper lug on the inlet end.

Heat insulation was applied to the test section after surface thermocouples and voltage taps were installed. One inch of laminated asbestos was first applied. Then six thermocouples were placed on the outside of this material at the following locations: one, an inch before the copper lug at the inlet; one each at 1/2, 19-13/16, 55-1/4 and 71-1/2 in. from the inlet lug; and one, an inch from the copper lug at the outlet. These couples were used to determine the heat loss.

19

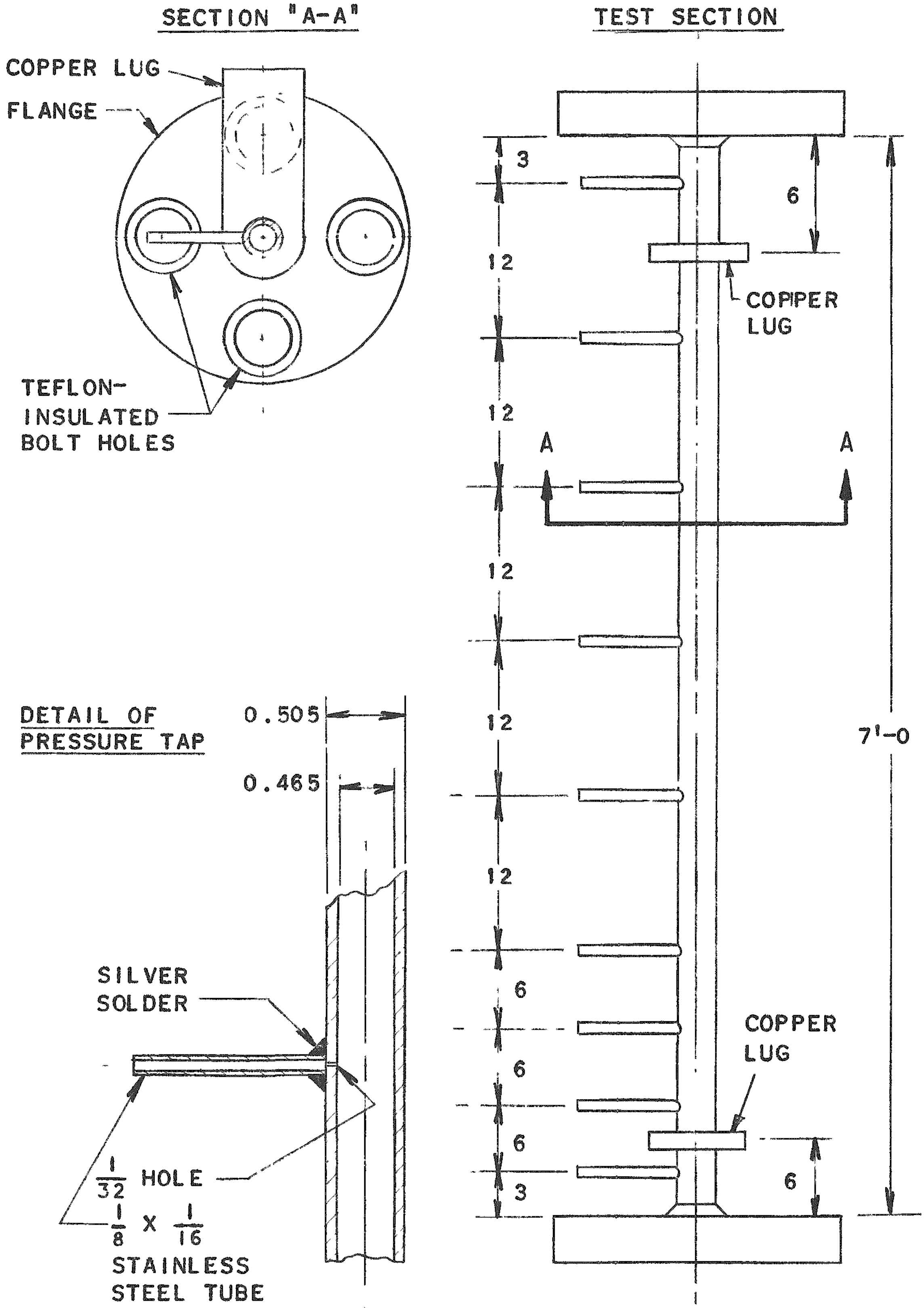

FIGURE 9 LOCATION OF PRESSURE TAPS ON TEST SECTION

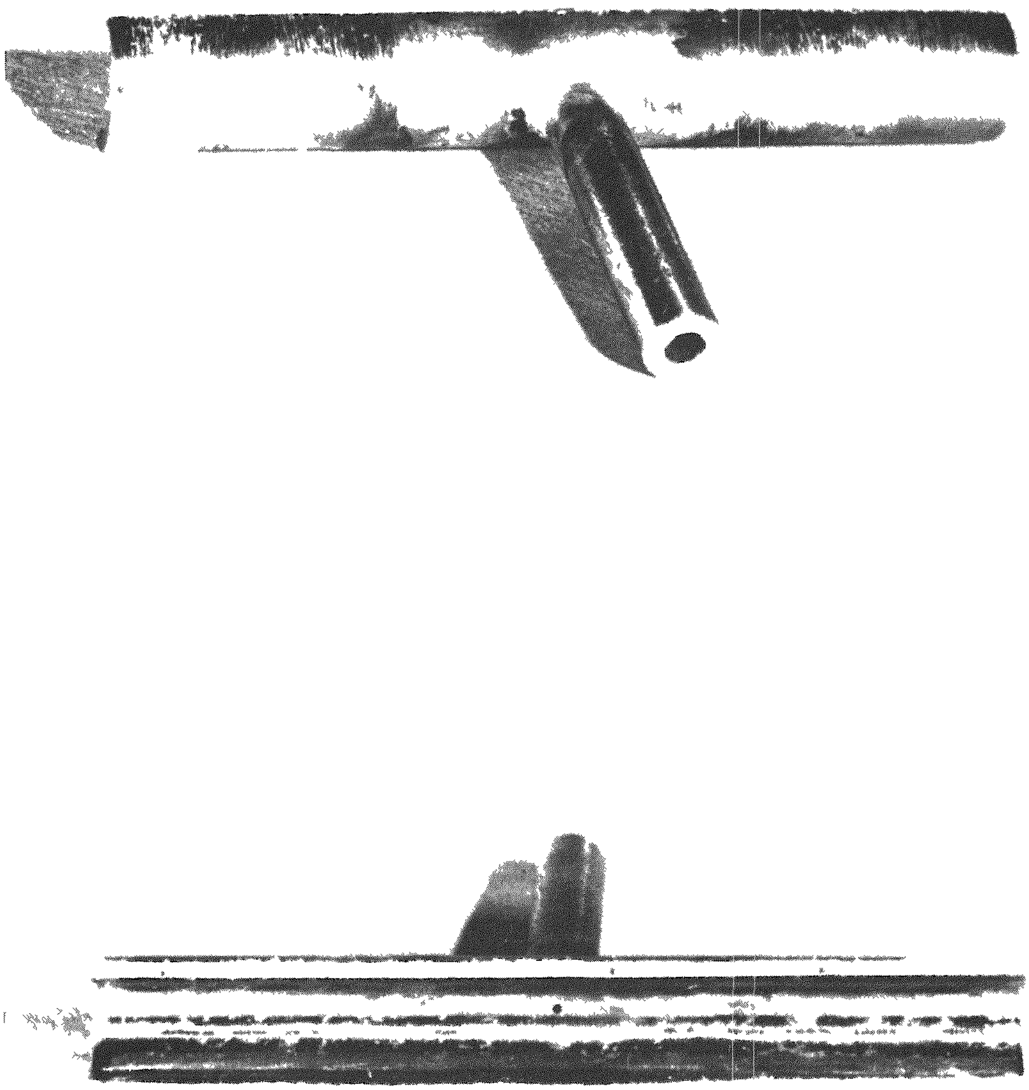

FIGURE 10 CUT-AWAY VIEW OF SAMPLE PRESSURE TAP

21

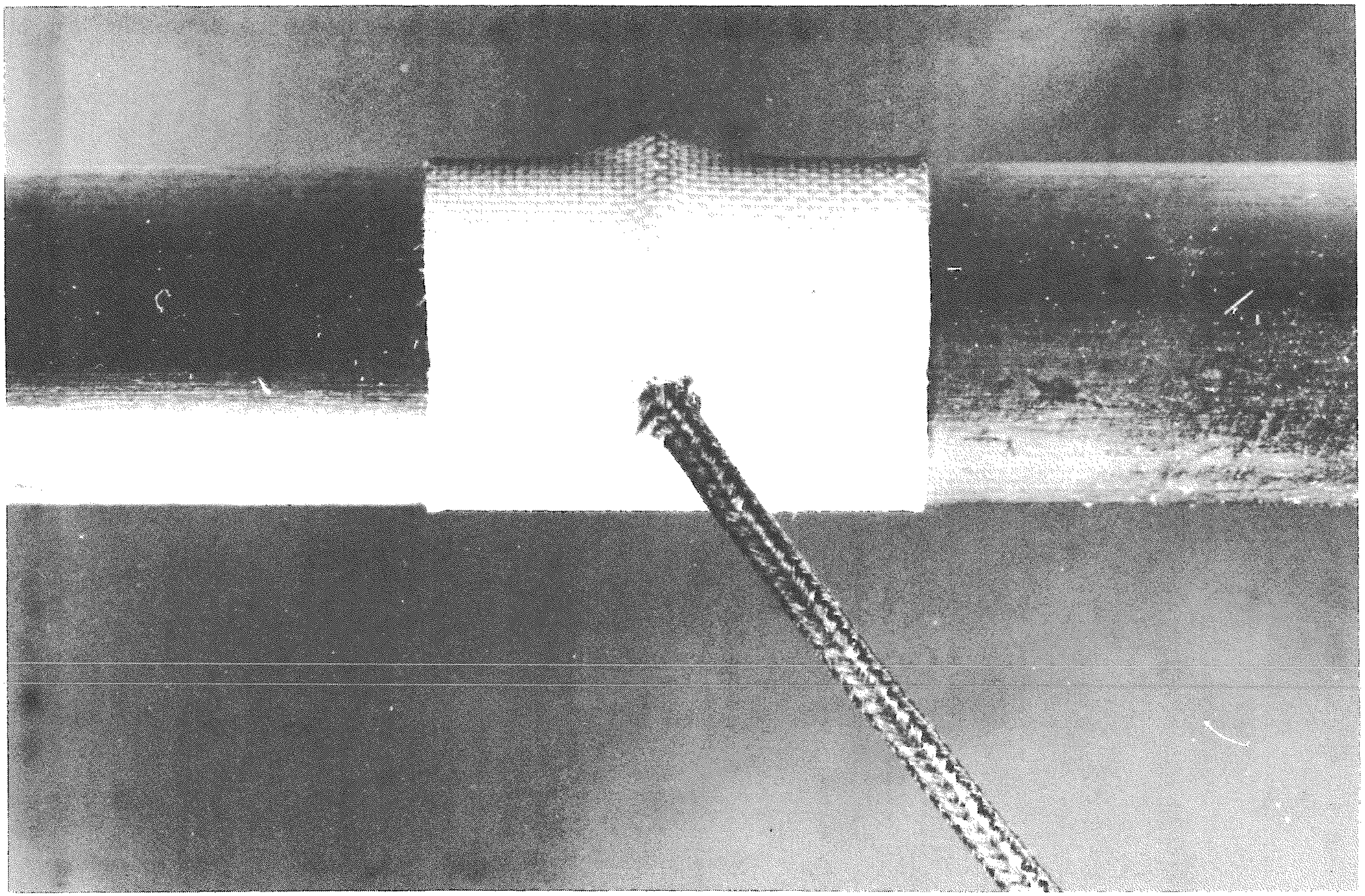

FIGURE 11 THERMOCOUPLE INSTALLATION

C. Temperature Measurement

The inlet and outlet water thermocouples were lead from the test section through individual lengths of copper shielding directly to a Leeds and Northrup Portable Precision Potentiometer. An ice junction was used as the reference junction for the potentiometer.

The wires of the forty-eight thermocouples used to measure the wall temperature of the test section were led through individual lengths of copper shielding to a 2-inch square duct and then to a junction box that was kept at room temperature. Here the wires were connected to thermocouple lead wires of the same material and led through a conduit to a Brown, Forty-Eight Point Electronic Precision Temperature Indicator. The instrument operated over 0-300F and 300-700F temperature ranges and provided its own room temperature compensation.

D. Pressure Measurement

Pressure drop measurements were made with four 60-inch U-tube manometers connected as shown in Fig. 12. Two stainless steel wells were constructed of 6-inch Schedule 40 pipe, so that the four manometers provided eight simultaneous pressure drop readings. The first four readings, of course, were all referenced to the first pressure tap, while the last four were referenced to the fifth pressure tap.

Pressure measurements were made with a precision Bourdon-type gage at the eighth pressure tap, located 3 in. upstream from the outlet power lug. During part of the experiment, a gage was installed at the first pressure tap as a check on the pressure drop measurements. Atmospheric pressure was observed on a mercury barometer.

The power reaching the test section from the three welding transformers previously described was measured with a calibrated wattmeter (Weston Model 432), which received its voltage from a step-up transformer (Westinghouse Type PV-130 Potential Transformer, 5, 4 and 2 to 1 ratios) and from either of two current transformers (Westinghouse Type U-5, 1500 to 5 amperes, Style 824238; and Type CT-2.5, 600 to 5 amperes, Style 1435495A), depending upon the current range in use.

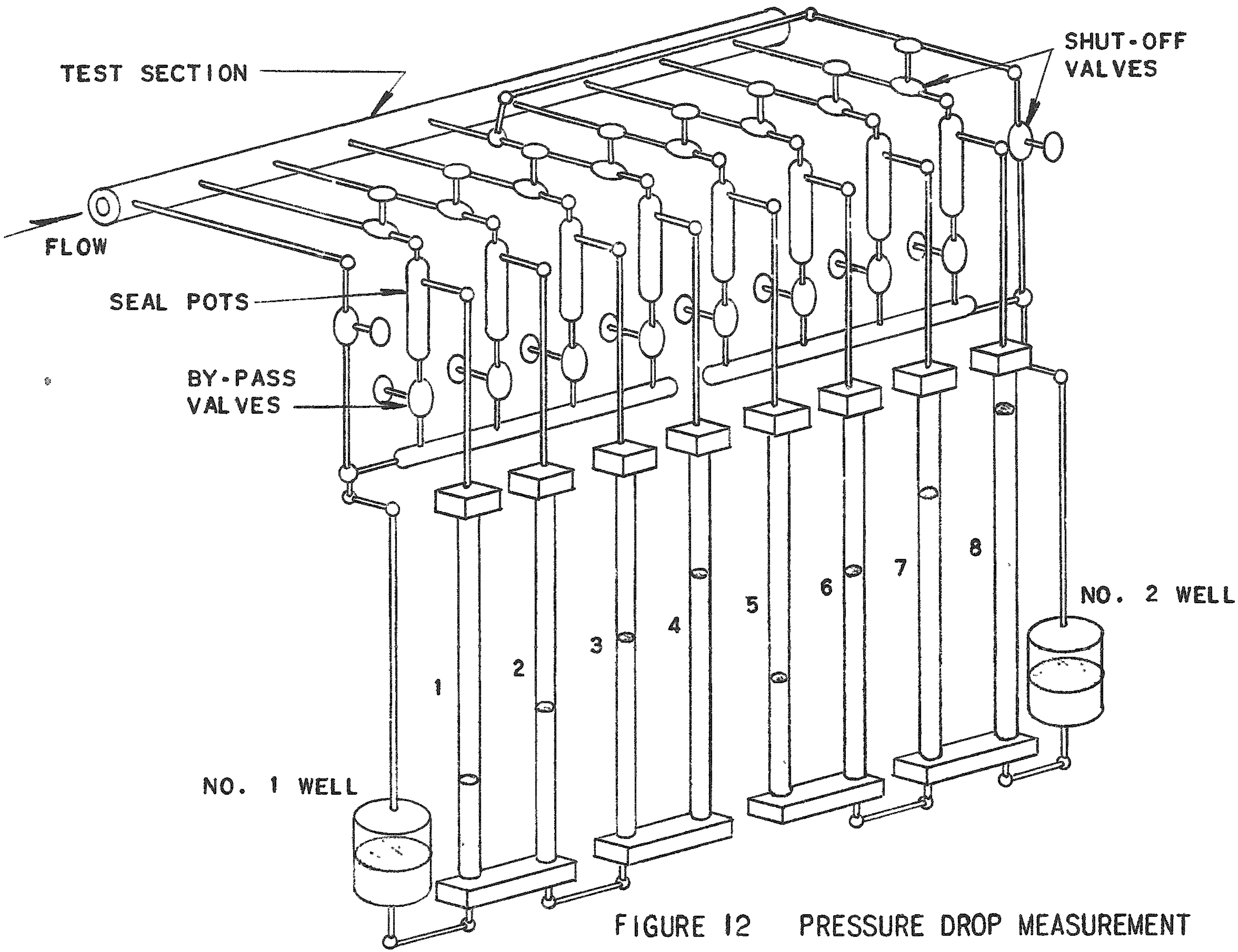

FIGURE 12 PRESSURE DROP MEASUREMENT

24.

IV. EXPERIMENTAL PROCEDURE AND TECHNIQUES

A. General

The test runs were made by setting a constant flow rate by means of the air-operated controller, maintaining the outlet pressure at the desired level (45, 90, 120, 150, 200 psia) manually with an exhaust throttle valve, setting the power at a particular level [5×10^4, 10×10^4, 15×10^4, 20×10^4, 25×10^4 Btu/(hr)(sq ft)], and adjusting the inlet temperature to the test section to cause boiling to begin at the proper point along the tube.

Equilibrium conditions were established for each run and held for a period of one-half hour before the data were recorded.

At the end of each week a check was made to determine whether or not scaling had taken place; no evidence of scale was observed.

Water quality was examined daily. The pH was kept at about 7 and the water resistivity was kept above 100,000 ohm-cm.

Re-runs were made periodically to determine reproducibility. Figure 13 shows a typical case of a re-run comparison.

B. Heat Loss

Previous (8) tests on a 1/2 in. OD test section, insulated in an identical manner, established the soundness of the insulating techniques. The heat loss from the section mounted to 0.1% at an operating power of 50 kw.

Heat balances were made where the observed power readings were checked against the product of measured flow, specific heat, and observed temperature rise. The instrument error plus power factor error thus observed was of the order of 3%. Typical data are given in Table I.

C. Heat Flux Distribution

It was assumed that the heat flux along the tube was uniform and, therefore, that the rate of steam generation along the tube was constant from the inception of boiling to the end of the heated length. Voltage measurements were made along the section during heating in an effort to verify this assumption; typical results are shown in Fig. 14. It is seen that the voltage drop was linear and, therefore, the heat generation was uniform.

25

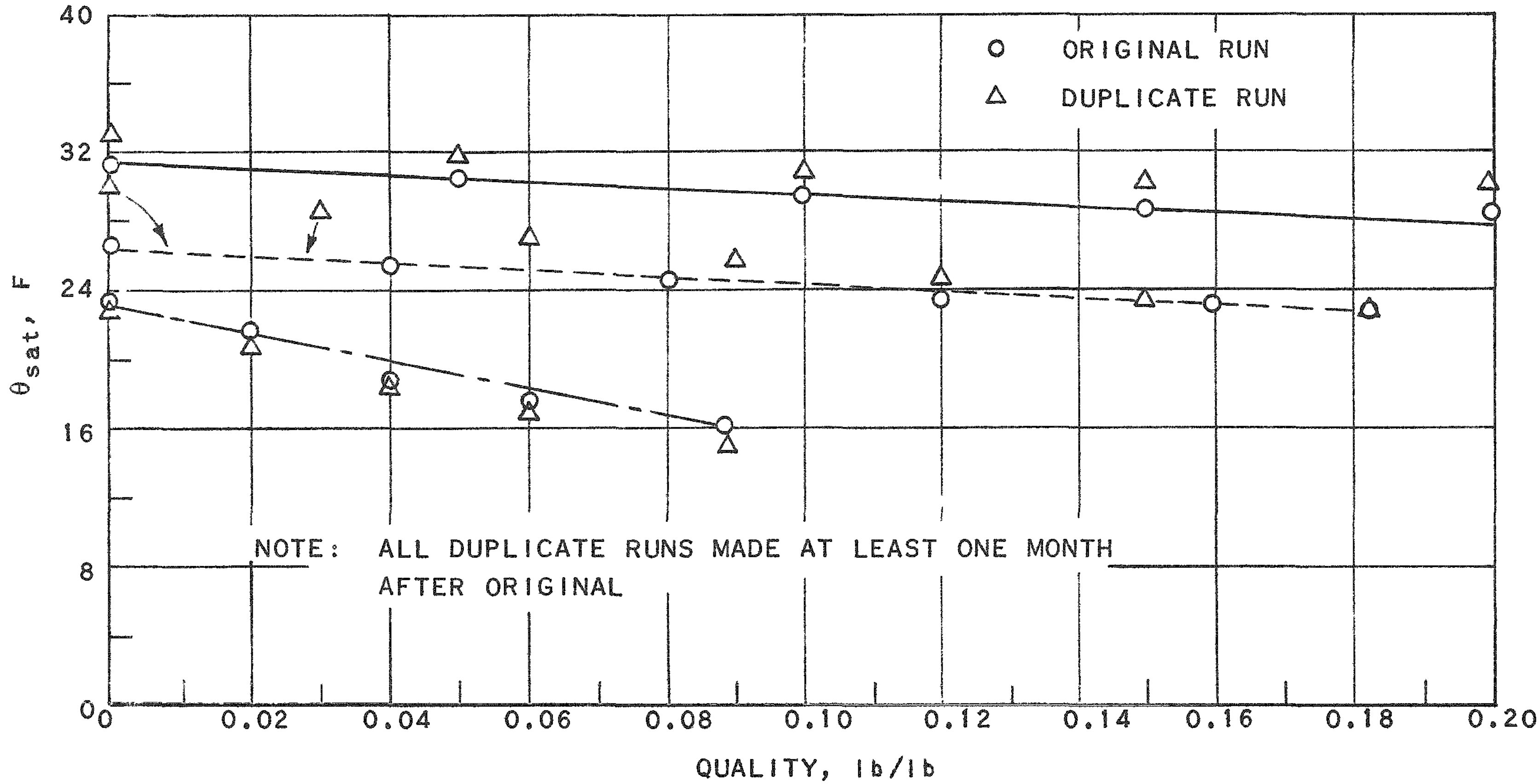

SYMBOL	PRESSURE psia	HEAT FLUX Btu/(hr)(sq ft)	RUN NO.
———	120	250,000	115
— — —	120	200,000	113
—·—	90	150,000	87

FIGURE 13 COMPARISON OF DUPLICATE RUNS

Table I

HEAT BALANCE DATA

Date	Power, kw	Flow, lb/min	c_p, Btu/(lb)(F)	t_{in}, F	t_{out}, F	Δt, F	Power, kw	ΔPower, kw	Error, %
11/17/53	21.15	9.90	1.00	107.1	225.8	118.7	20.60	0.55	2.6
	21.00	19.9	1.00	137.0	195.0	58.0	20.30	0.70	3.3
	21.15	24.6	1.00	144.0	191.0	47.0	20.35	0.80	3.8
11/27/53	21.15	24.7	1.00	144.0	191.0	47.0	20.40	0.75	3.6
	21.00	40.7	1.00	153.0	181.5	28.5	20.40	0.60	2.9
	21.10	41.8	1.00	155.0	183	28.0	20.50	0.60	2.9
1/18/54	21.10	25.0	1.00	145.0	191.5	46.5	20.40	0.70	3.3
	21.15	30.0	1.00	148.0	187.5	39.5	20.80	0.35	1.7
	21.00	40.0	1.00	155.0	184.0	29.0	20.40	0.60	2.9

87

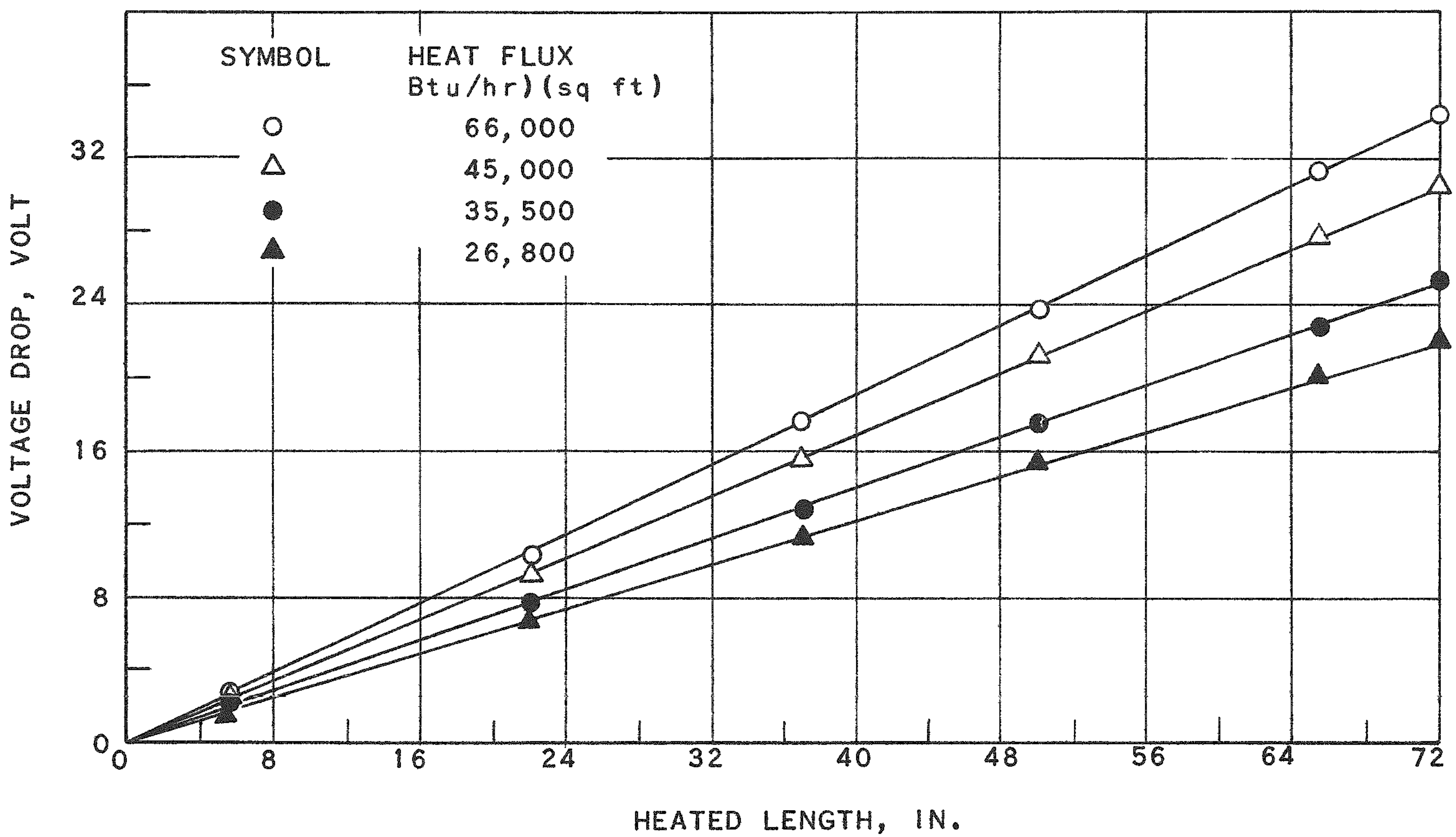

FIGURE 14 VOLTAGE DROP ALONG TUBE

The uniformity of the heat generation per unit length did not extend to the immediate vicinity of the pressure taps. An extensive mathematical investigation has not been made for this region since the points were not used for analysis.

D. Pressure Drop

Pressure drop data were taken for each run so that the saturation temperature at each point along the tube could be evaluated. No analysis of the pressure drop data was attempted.

E. Temperature Measurements

Thermocouples were located in the fluid stream before and after the heated section. The exit thermocouple was located between pressure taps so that the pressure and, hence, the saturation temperature, could be found by interpolation. In all cases the exit thermocouple indicated a temperature within one degree of saturation.

The surface thermocouples were read from a forty-eight point indicator. The temperatures were plotted directly on graph paper, as shown in Fig. 15, so that a temperature traverse of the tube was immediately available. Once equilibrium had been established there was a remarkable absence of fluctuations until qualities of the order of 60% were reached. As qualities above 60% were reached, the temperature fluctuated by hundreds of degrees and burnout finally occurred at a quality near 70%.

F. "Wilson Plots"

In an effort to detect any scaling that might interfere with the heat transfer measurements "Wilson Plots"[10] were made at the end of each week. This did not coincide with the time at which the system was drained and recharged.

A "Wilson Plot" is a form of plotting heat transfer data that was introduced by E. E. Wilson in 1915. Although the Dittus and Boelter[11] or Colburn[12] relation was not known at that time, Wilson found, by trial and error, that he could obtain the water side coefficients of heat transfer by plotting $\frac{1}{U}$ vs $\frac{1}{V^{0.82}}$ (where V refers to velocity) on rectangular coordinate paper and extrapolating to infinite velocity.

The validity of this form, based on the assumption used, can be demonstrated as follows. Assume that the Colburn[12] relation holds throughout the turbulent region:

$$\frac{h_c D_e}{k_f} = C_1 \left[\frac{\gamma V D_e}{\mu f}\right]^{0.8} \left[\frac{\mu f\, c_p}{k}\right]^{1/3}$$

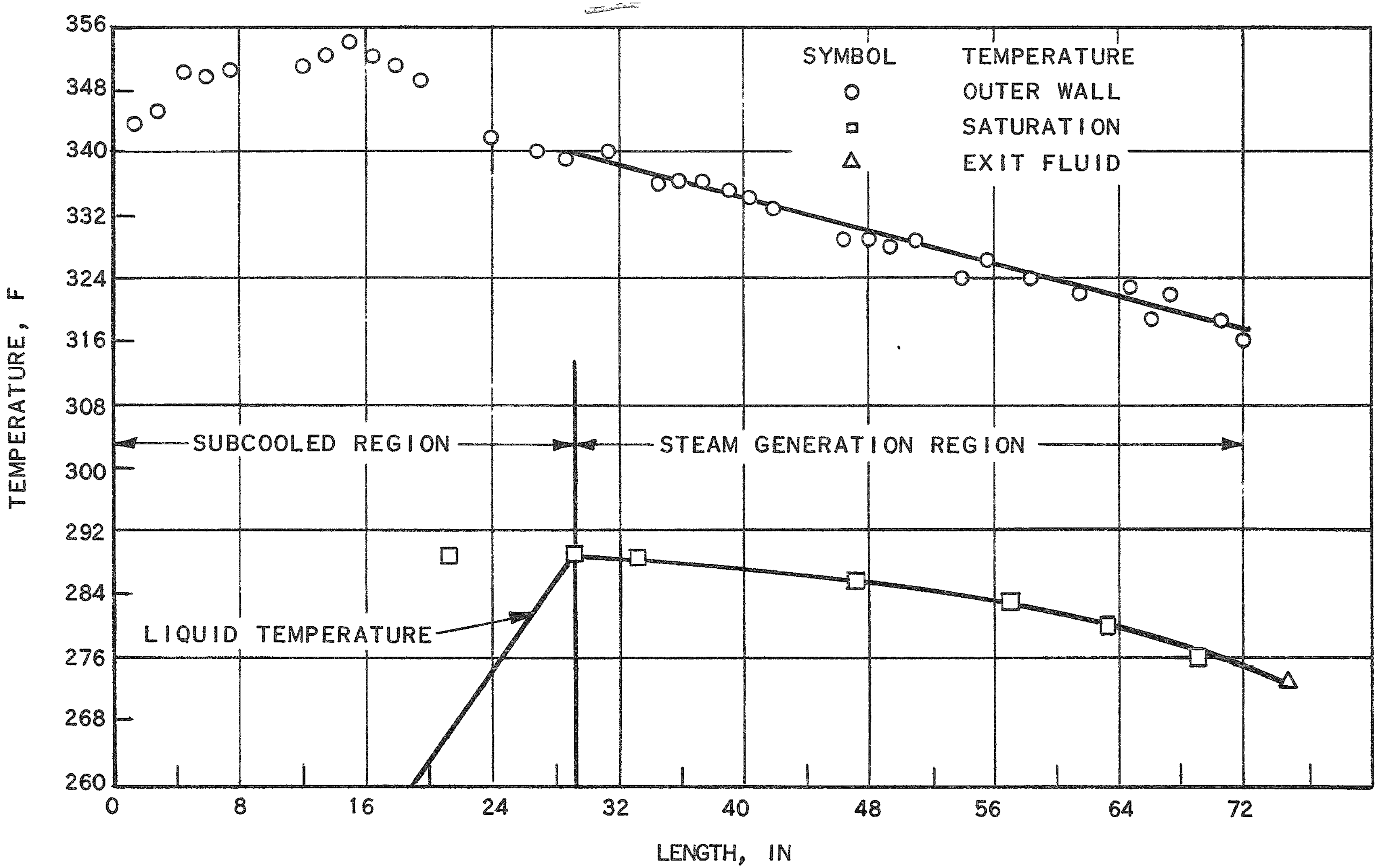

FIGURE 15 TYPICAL TEMPERATURE DATA

In this case D_e is constant, and since the average fluid temperature was kept constant by adjusting the flow and heat input, k, γ, μ_f, and c_p were also constant. Therefore,

$$h_c = C_2 \ V^{0.8}$$

Assuming that $r_1 \approx r_2$ and, therefore, a slab geometry can be used for the sake of brevity, the over-all coefficient of heat transfer can be expressed as:

$$\frac{1}{U} = \frac{1}{h_c} + \frac{s}{k} + \frac{1}{h_{sc}}$$

Since $h_c = C_2 \ V^{0.8}$

$$\frac{1}{U} = \frac{1}{C_2 \ V^{0.8}} + \frac{s}{k} + \frac{1}{h_{sc}}$$

As V tends to ∞, $\frac{1}{C_2 \ V^{0.8}}$ tends to zero; therefore, by extrapolating to zero, the intercept yields the value of $\frac{s}{k} + \frac{1}{h_{sc}}$. Since $\frac{s}{k}$ is known, the value of h_{sc} can be found. Figure 16 shows the results of a typical "Wilson Plot." No evidence of scale was found.

G. Comparison With The Colburn Correlation

Runs were made with an all-liquid system and the measured coefficients were compared with coefficients calculated from the Colburn[12] equation:

$$\frac{h_c D_e}{k} = 0.023 \ (N_{Re})^{0.8} \ (N_{Pr})^{1.3}$$

Figure 17 shows the comparison of the measured coefficients with the calculated coefficients.

31

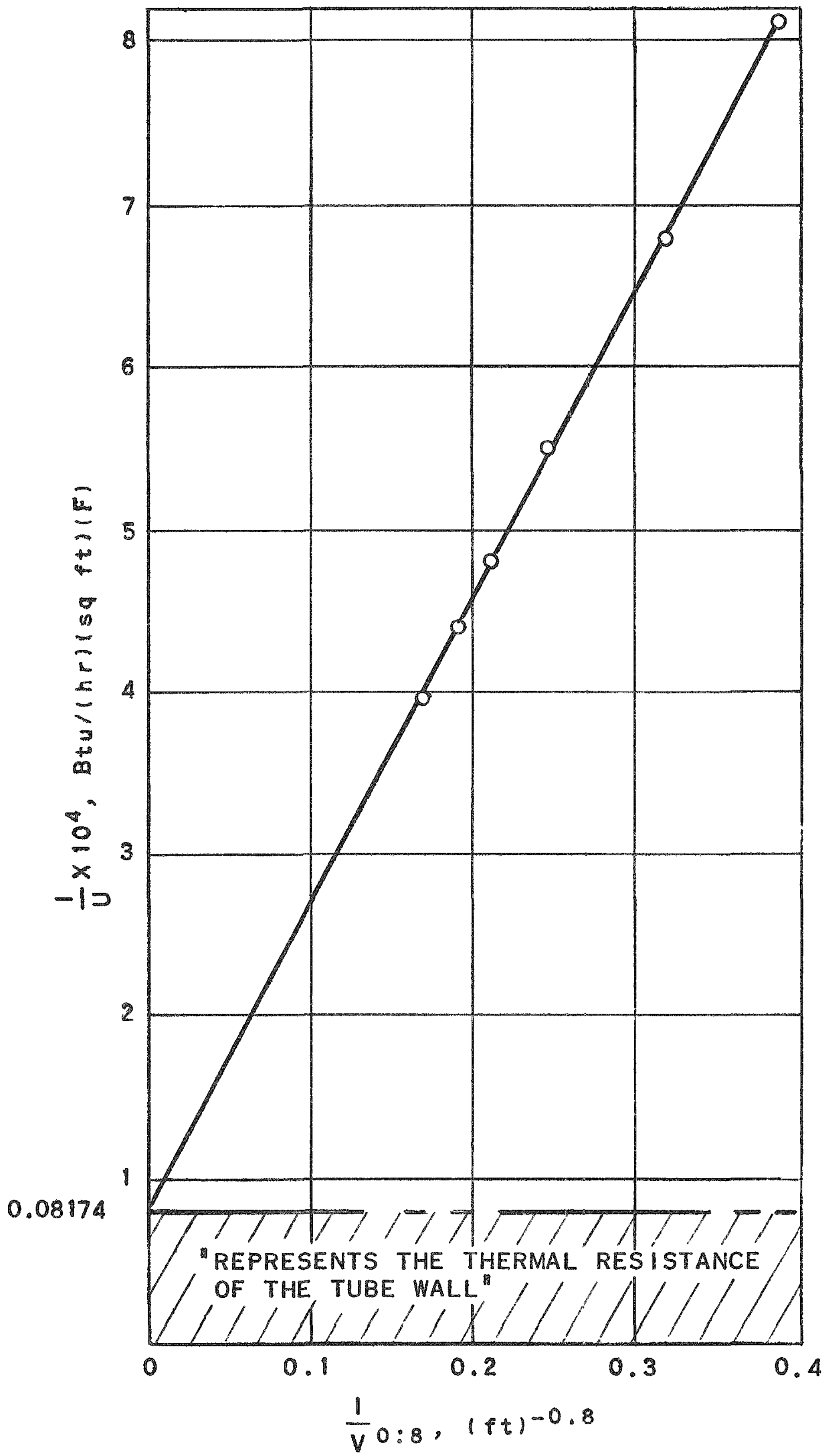

FIGURE 16 TYPICAL WILSON PLOT

32

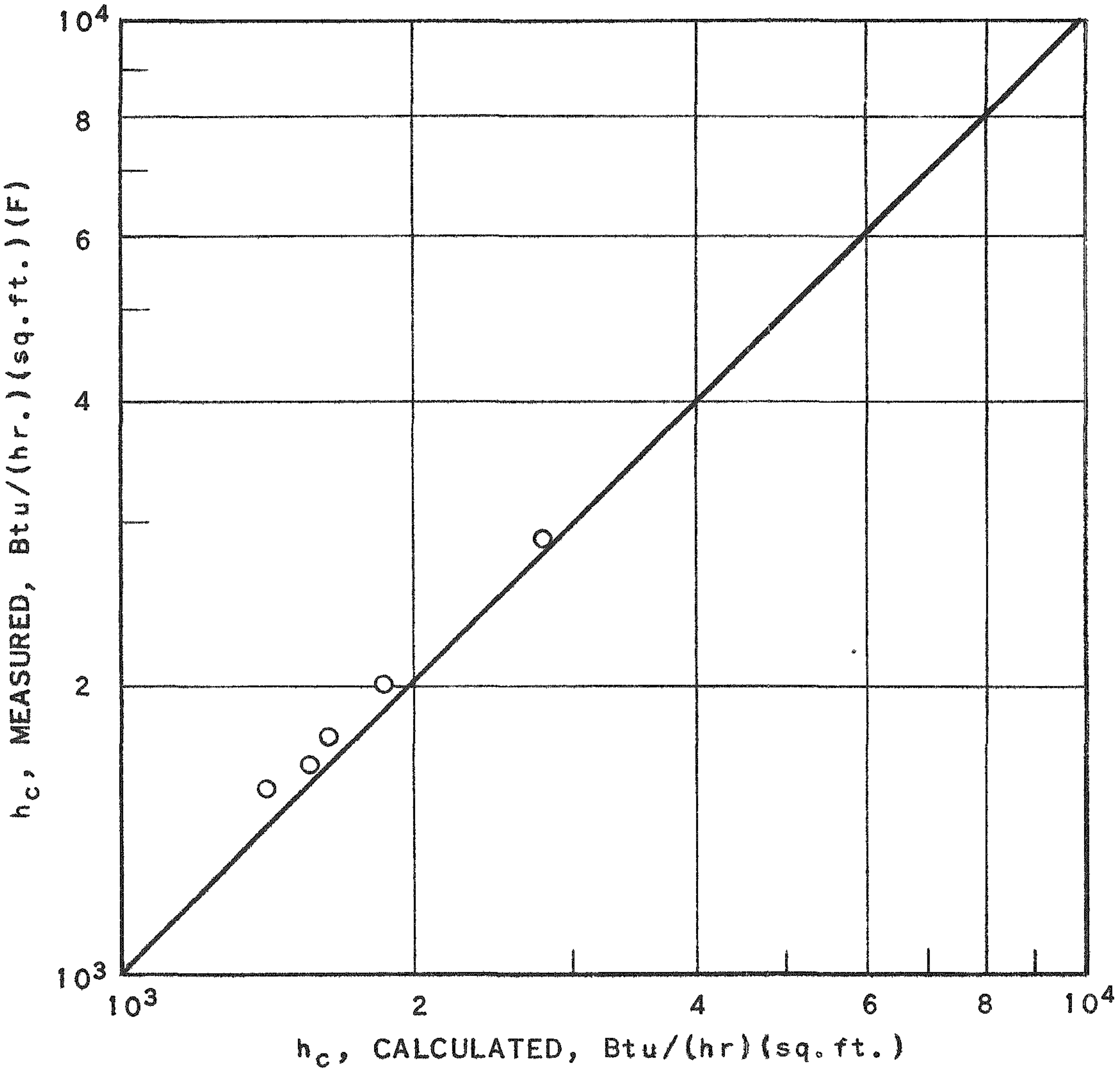

$$h_c = 0.023 \frac{k}{D_e} \left[N_{Re}\right]^{0.8} \left[N_{Pr}\right]^{\frac{1}{3}}$$

FIGURE 17 COMPARISON WITH COLBURN RELATION

V. DISCUSSION

A. General

The mechanism of boiling is understood only in a qualitative way and the essential variables are not completely defined. Since there are no mathematical expressions as yet formulated to show the relative importance of the variables one must rely, to some extent, on intuition in trying to formulate a correlation. It is, of course, possible to guess the variables and apply the methods of dimensional analysis to obtain dimensionless parameters. Unfortunately, it is difficult, if at all possible, to find the proper variables and to distinguish their relative importance. In fact, one has to be careful how he solves for the exponents, since it is possible to get different dimensionless parameters using the same set of variables.

However, there are well-known dimensionless groups that seem to have physical significance. The successful use of these has had a large part in the development of fluid flow and heat transfer knowledge.

In this case, a rather general correlation was attempted with the hope that it might prove useful for correlating the data of other investigators.

The dimensionless parameters used were chosen after a rather thorough search of the literature, many attempts at the use of dimensional analysis, and various trials at forming a correlation.

In the final analysis values of h, at constant quality and at constant heat flux, were plotted against mass flow, using pressure as a parameter. Next, values of h, at constant quality and mass flow, were plotted against heat flux, using pressure as a parameter.

These data could be represented by straight lines when plotted on log-log paper. Since dimensionless groups were to be formed, only the slope of these lines were used. The dimensionless parameters were then formed and the data for each pressure were plotted on rectangular coordinate paper with quality as a parameter. Examination of the data indicated that the film coefficient varied linearly with quality up to about 40% and that the slope depended on the pressure. A function, of the form $1 + mx$, was obtained where the slope, m, was a pressure function. The correlation so formed was then compared with the experimental data as shown in Fig. 25.

B. Effect of Flow

The data were assembled in graphical form and points were selected at a quality of 5%. The measured heat transfer coefficient was plotted against flow rate at a constant heat flux with pressure as a parameter. Figure 18 shows a typical plot at a heat flux of 250,000 Btu/(hr)(sq ft) for pressures of 45, 90, and 120 psia. The lines were parallel and the slope equal to 0.344.

SYMBOL	PRESSURE	HEAT FLUX Btu/(hr)(sq ft)	QUALITY lb/lb
○	45	250,000	0.05
△	90	250,000	0.05
□	120	250,000	0.05

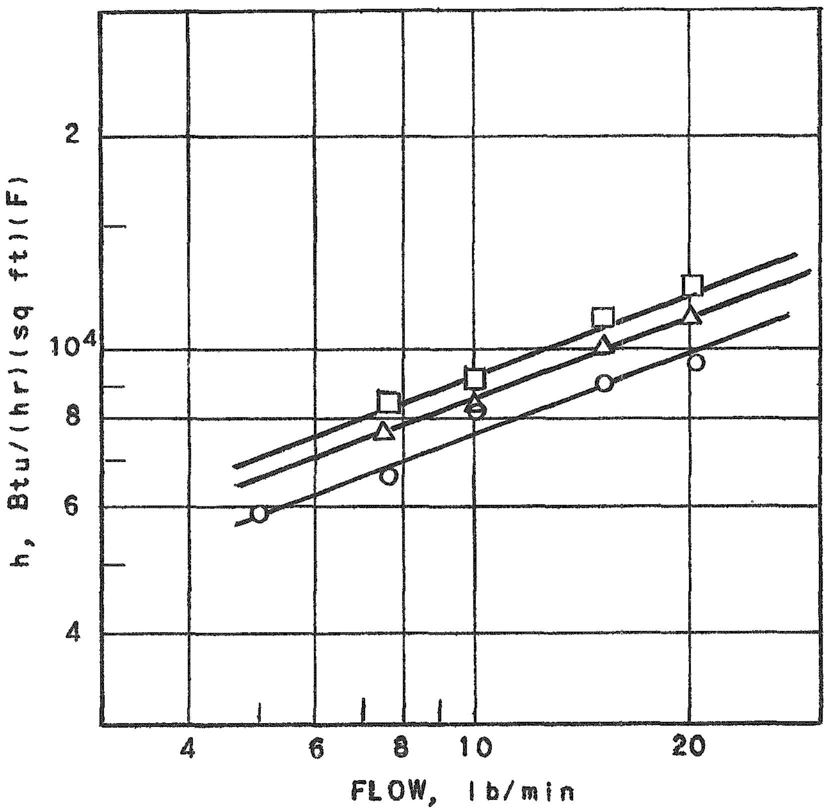

SLOPE OF LINES EQUALS 0.344

FIGURE 18 VARIATION OF FILM COEFFICIENT WITH FLOW

C. Effect of Heat Flux

The heat transfer coefficients were then plotted against heat flux at a constant flow with pressure as a parameter. The lines were parallel with a slope equal to 0.464. Figure 19 shows the results of one such plot at a flow rate of 7.5 lb/min for pressures of 45, 90, and 120 psia.

D. Effect of Quality

Examination of the data indicates that, to a first approximation, θ_{sat} varies linearly with the quality and the slope is a function of the pressure. Figure 20 shows the trend of the slopes with pressures for runs at 250,000 Btu/(hr)(sq ft) heat flux and 7.5 lb/min flow rate.

E. The Dimensionless Group N_{Nu}

The data were correlated by means of four dimensionless groups. The first of these was the Nusselt Number N_{Nu}. The thermal conductivity of the liquid is used in evaluating the number.

F. The Dimensionless Group $C\left[1 + a\left(\frac{V_{fg}}{V_f}\right)^b x\right]$

The data indicated that the film coefficient varied linearly with quality and that the slope of the line depended upon pressure. The second dimensionless group chosen was $C\left[1 + a\left(\frac{V_{fg}}{V_f}\right)^b x\right]$, which has the form of an equation for a straight line and where the slope, $a\left(\frac{V_{fg}}{V_f}\right)^b$, is a function of pressure. This straight line relationship does not hold when the quality exceeds 0.40.

G. The Dimensionless Group N_B

The third of the dimensionless groups chosen was N_B. Davidson et al.,[3] made mention of the dimensionless group N_B and used its magnitude as a measure of overheat conditions. They arrived at this group by considering Jakob's free boiling parameter, $\left(\frac{q''}{\rho_g h_{fg} D_b f}\right)$. This group can also be arrived at by the methods of dimensionless analysis.

In the case where net steam is generated, as is reported here, the group can be considered as the ratio of total heat transferred to net steam generated times a ratio of diameter to length. This can be demonstrated as follows:

$$\frac{q''}{Gh_{fg}} = \frac{q\ D^2}{L\ D\ m\ 4\ h_{fg}}$$

$$= \frac{q}{m\ h_{fg}} \cdot \frac{D}{4L}$$

SYMBOL	PRESSURE psia	FLOW RATE lb/min	QUALITY lb/lb
○	45	7.5	0.05
△	90	7.5	0.05
□	120	7.5	0.05

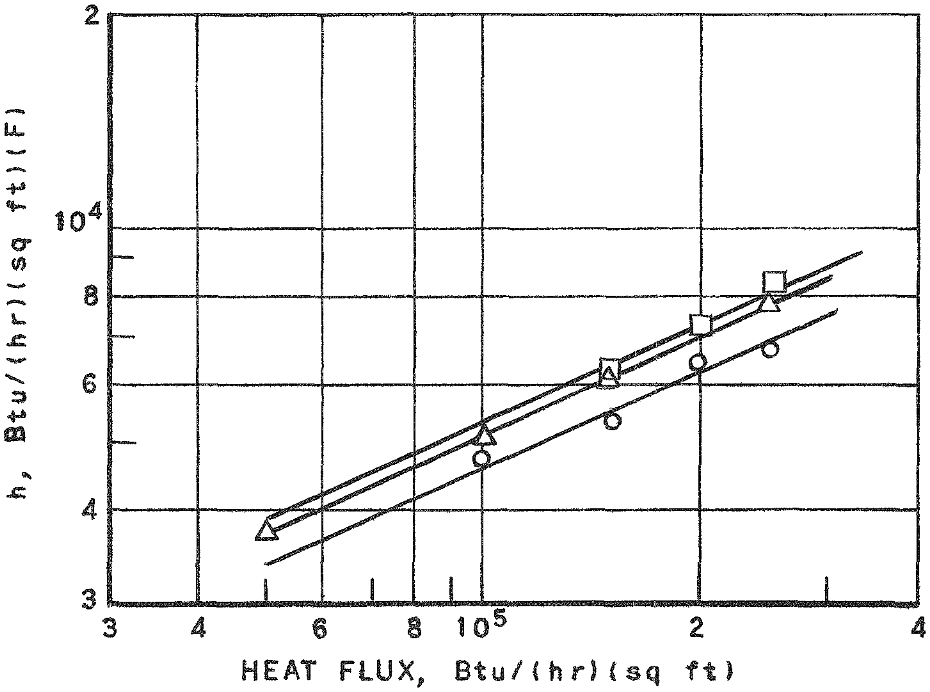

SLOPE OF THE LINES EQUALS 0.464

FIGURE 19 VARIATION OF FILM COEFFICIENT WITH HEAT FLUX

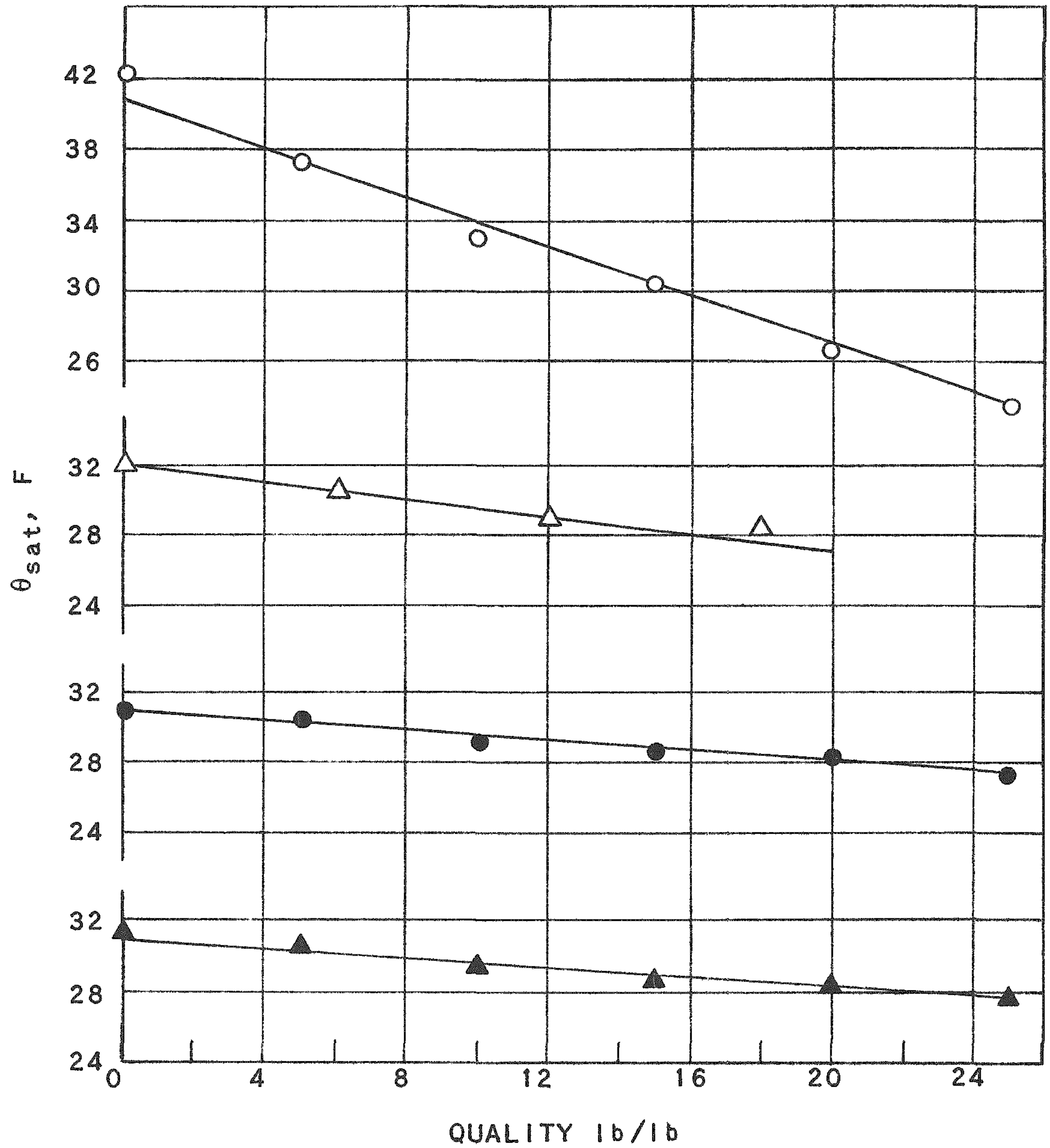

SYMBOL	PRESSURE psia	HEAT FLUX Btu/(hr)(sq ft)(F)
○	45	250,000
△	90	250,000
●	120	250,000
▲	150	250,000

FIGURE 20 VARIATION OF θ_{sat} WITH QUALITY

Since the heat generation was uniform along the tube length, the ratio of the heat transferred to steam generated was constant along the tube and, therefore, the total q was significant and the D/4L ratio could be put into the constant. The ratio then has physical significance that is easily understood. Unfortunately, this reasoning cannot be extended to the local or subcooled boiling region since any steam formed is quickly condensed in the main stream. At the same time, the dimensionless group $\frac{q''}{Gh_{fg}}$ does seem to have some importance in the region of local boiling.

If the group is to have any general physical significance, it must be considered as a measure of the intensity of the boiling phenomenon and thereby relates the amount of heat to be transferred at a given cross section to the ability of the stream to absorb it. With this reasoning it may be possible to expand the area in which one might predict conditions with confidence.

H. The Dimensionless Group N_{Re}

The fourth dimensionless group chosen was the Reynold's Number, N_{Re}. The Reynold's Number is used extensively in the fields of fluid flow and heat transfer. As is true of all dimensionless groups, there is difficulty in determining which physical properties to use.

It has been rather definitely established that in turbulent flow of a fluid through a pipe there exists a laminar boundary layer next to the surface. The thickness of the boundary layer is a function of Reynold's Number.[7]

For the boiling case the situation is more complicated in that the liquid boundary layer is constantly being disrupted by the formation of bubbles. However, the high heat transfer rates are possible only when there is a liquid layer against the wall, for once the wall is dry it cannot, for all practical purposes, be re-wet. As a gas film tends to form, the heat transfer rates decrease sharply and the surface temperature begins to fluctuate. If a gas film is allowed to form on the surface of an electrically-heated tube at heat fluxes such as are reported here, the tube burns out. Since the mechanism is controlled by the liquid, the viscosity of the liquid is used in the expression of the Reynold's Number.

I. Formulation of the Correlation

The form of the equation chosen was

$$\frac{hD_e}{k} = C\left[1 + a\left(\frac{V_{fg}}{V_f}\right)^b x\right]\left(\frac{q''}{Gh_{fg}}\right)^d \left(\frac{G\,D_e}{\mu_f}\right)^e$$

The data were put into this form in the following manner. From the slopes determined from Figs. 18 and 19:

$$h = C_{1g}\,(x,p)\,(q'')^{0.464}\,(G)^{0.344}$$

or

$$h = C_{1g}\,(x,p)\left(\frac{q''}{G}\right)^{0.464}(G)^{0.808}$$

There were then formed the dimensionless groups

$$\frac{h\,D_e}{k} = C_2\left[1 + a\left(\frac{V_{fg}}{V_f}\right)^{b} x\right]\left(\frac{q''}{Gh_{fg}}\right)^{0.464}\left(\frac{GD_e}{\mu_f}\right)^{0.808}$$

The data at each pressure were then plotted with the dimensionless group, N_{Nu} as ordinate and $(N_B)^{0.464}\,(N_{Re})^{0.808}$ as abscissa and with quality as a parameter as shown in Fig. 21, which is for a pressure of 90 psia. Some over-lapping of the data was caused by the limits of the experimental accuracy. The slopes of these lines were found to be equal to

$$C\left[1 + a\left(\frac{V_{fg}}{V_f}\right)^{b} x\right],$$

the function of quality assumed. These values were then cross plotted versus quality with pressure as a parameter as shown in Fig. 22. The lines are seen to be approximately straight with a common intercept. The slopes of these lines were then plotted against the ratio of V_{fg} to V_f, a pressure function, as seen in Fig. 23. From this function

$$C\left[1 + a\left(\frac{V_{fg}}{V_f}\right)^{b} x\right]$$

was determined to be

$$4.3\left[1 + 16 \times 10^{-4}\left(\frac{V_{fg}}{V_f}\right)^{1.64} x\right]$$

The resulting equation was, with a small modification,

$$\frac{h\,D_e}{k} = \left[4.3 + 5.0 \times 10^{4}\left(\frac{V_{fg}}{V_f}\right)^{1.64} x\right]\left(\frac{q''}{Gh_{fg}}\right)^{0.464}\left(\frac{G\,D_e}{\mu_f}\right)^{0.808}$$

or

$$N_{Nu} = \left[4.3 + 5.0 \times 10^{-4}\left(\frac{V_{fg}}{V_f}\right)^{1.64} x\right](N_B)^{0.464}\,(N_{Re})^{0.808}$$

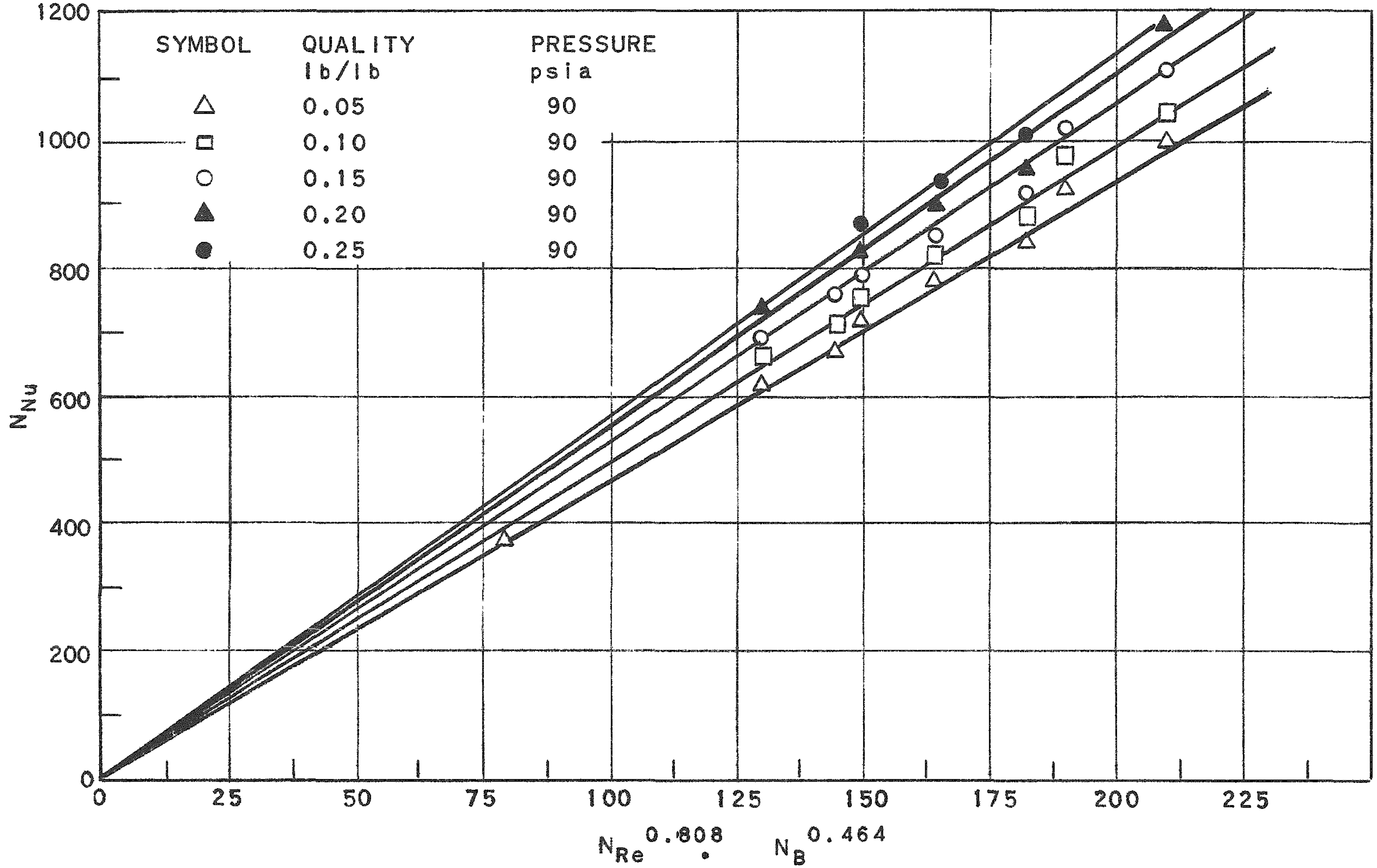

FIGURE 21 ESTABLISHING VALUE OF $C\left(1 + a\left(\frac{V_{fg}}{V_f}\right)^b X\right)$

4-1

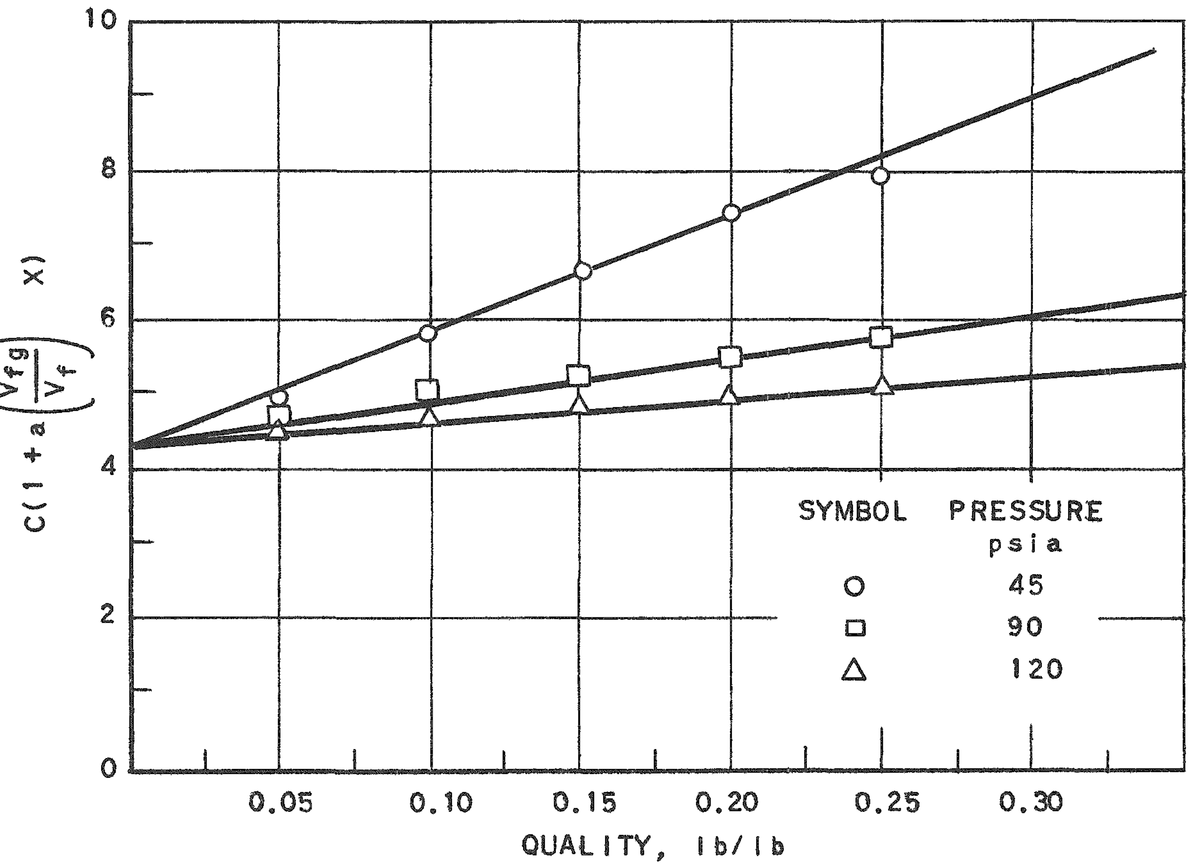

FIGURE 22 VARIATION OF $C\left(1+a\left(\frac{V_{fg}}{V_f}\right)^b X\right)$ WITH QUALITY

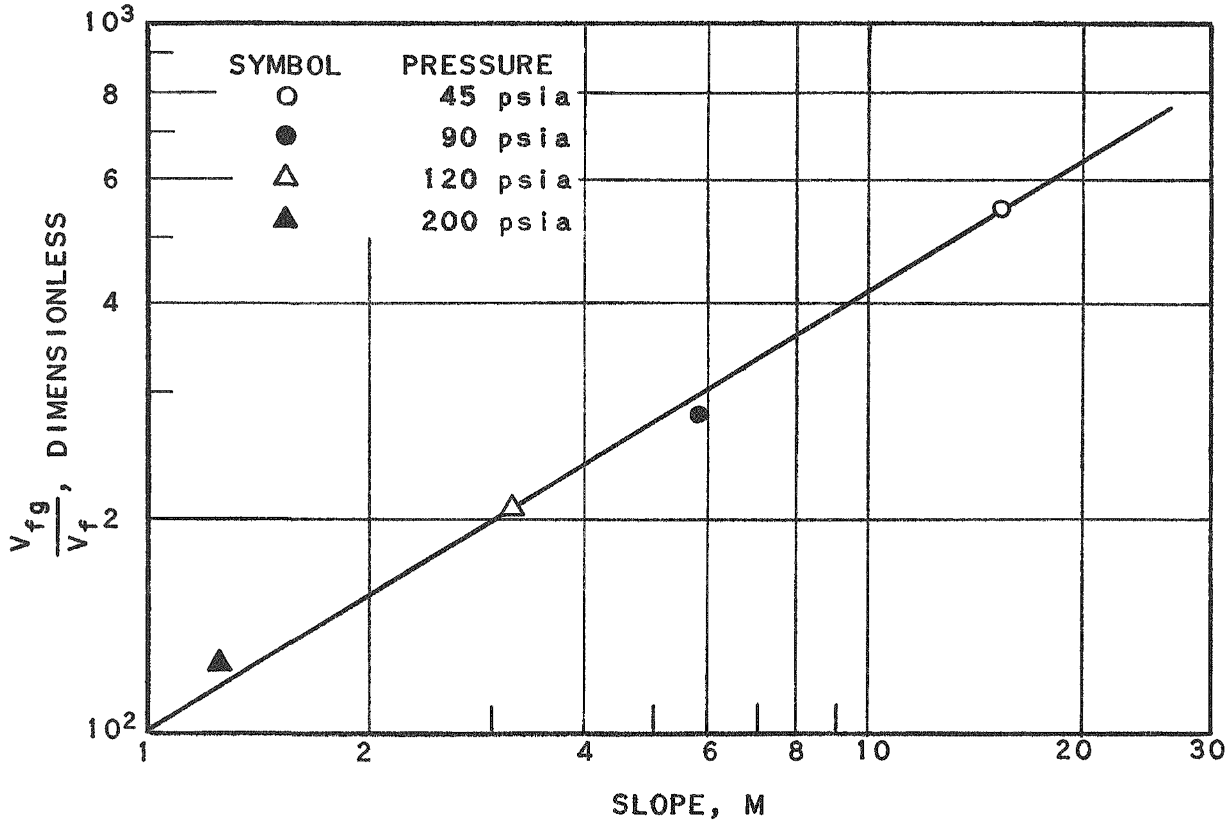

FIGURE 23 ESTABLISHING VALUE OF $a\left(\frac{V_{fg}}{V_f}\right)^b$

A comparison of measured values versus calculated values of the Nusselt Number is shown in Fig. 25. The root mean square value of scattering is 10%.

J. Evidence of Vapor Film Formation

A limited number of runs were made where the quality was higher than 40%. Figure 24 shows the resulting θ_{sat} for one run. Unfortunately, the test section burned out at a quality near 70% and damage to the equipment precluded the experiment. Too few runs were made at high qualities to be used quantitatively in the correlation. At burnout, which occurs at a quality near 70% for a heat flux of 250,000 Btu/(hr)(sq ft), θ_{sat} is of the order of 1500F which is between 30 and 50 times the minimum θ_{sat}. Since this is of the same order as could be expected of a gas film, it may be concluded that between qualities of 50 and 70% of the film changes from liquid to vapor. Once the vapor is formed, burnout occurs in a matter of a second at these heat fluxes.

K. Extension of the Correlation

Mr. R. Rohde of Argonne National Laboratory has, in conjunction with the author, used the parameter arrived at in this report to correlate local boiling data taken at Massachusetts Institute of Technology(13) and University of California, Los Angeles(14) on vertical sections. These data cover pressure ranges from 100 psia to 2500 psia and heat fluxes to 2.5×10^{-6} Btu/(hr)(sq ft). The form of the equation is

$$\frac{h\,D_e}{k} = \frac{C_1}{\ln \frac{1}{P_r}} \left(\frac{q''}{Gh_{fg}}\right)^a \left(\frac{G\,D_e}{\mu_f}\right)^b$$

The exponents a and b are the same as those arrived at in this report, but the coefficients are different. For the University of California, Los Angeles, data C_1 is equal to 6 and for the Massachusetts Institute of Technology data the coefficient is 8.5. The mean value of scattering in these investigations is 25%. It may be that one should also use a Prandtl Number. This work is not yet complete, but it is interesting to note that the data are correlated by means of the dimensionless parameters described.

L. Limitations of the Experiment

1. Mass Velocity

A flow rate of 71 lb/(sec)(sq ft) was the minimum possible with the flow control system, pump, and pump motors that were used. Flow control was difficult at this low rate. Unfortunately, one lower flow rate was tried to get higher qualities and the tube burned out before a complete set of data could be obtained. The maximum heat flux would allow only low qualities at the high flow rates at higher pressures.

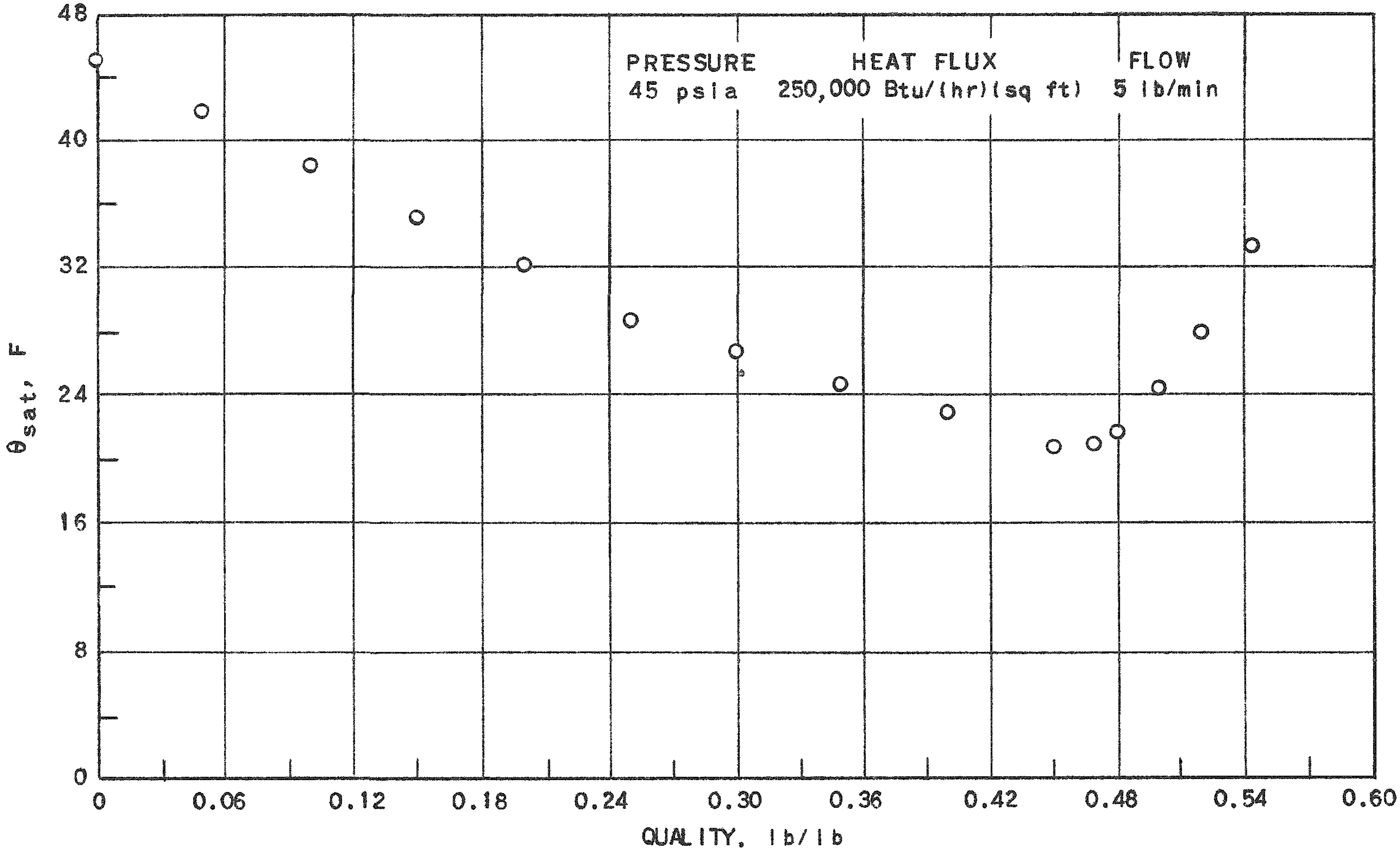

FIGURE 24 CHANGE IN θ_{sat} WITH QUALITY

+5

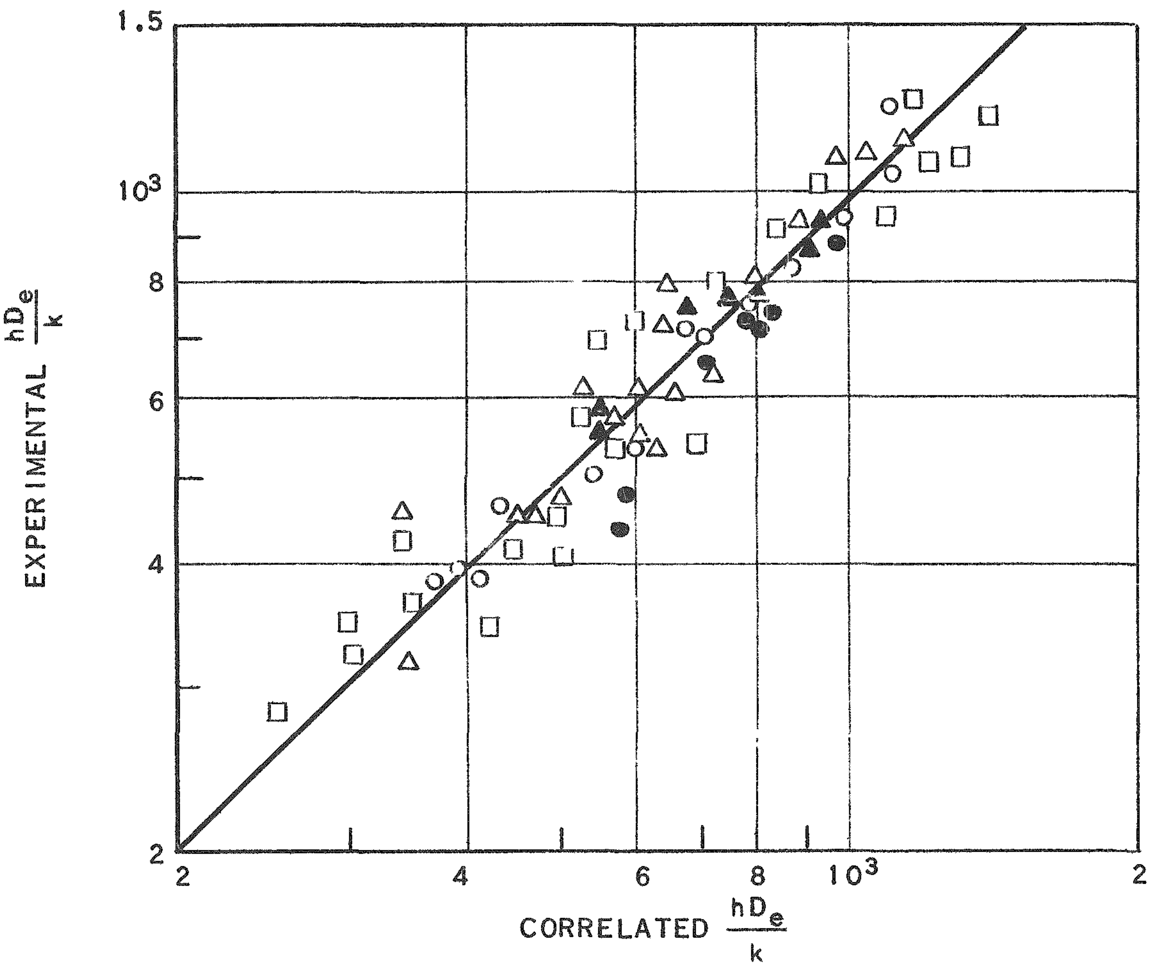

NOTE: EACH POINT REPRESENTS THE GRAVITATIONAL CENTER OF 3 DATA POINTS

FIGURE 25 COMPARISON OF EXPERIMENTS WITH CORRELATION

2. Absolute Pressure

A minimum pressure of 45 psia was chosen because of pressure drop characteristics. The pressure drop at high qualities became an appreciable part of the total pressure even at this pressure. A maximum pressure of 200 psia was chosen because of the power limitations. At any higher pressure only low qualities could be obtained and the preheater would not heat the fluid to the desired temperature.

3. Heat Flux

The maximum input to the test section from the power supply was 53 kw.

The exit quality obtained for each pressure and flow rate is given in Table II.

#7

Table II

EXIT QUALITY FOR EACH RUN
(In per cent)

Pressure, psia	Heat Flux, Btu/(hr)(sq ft)	Flow rate, lb/min					
		20	15	10	7.5	5	4
	250,000	4.4	13.3	20.7	28.4	54.4	X-Burnout
	200,000	7.7	10.7	16.9	22.7	43.2	
45	150,000	5.8	8.0	12.5	17.5	32.3	
	100,000	3.8	5.5	8.35	11.3	21.4	
	50,000	2.0	3.0		5.8	11.2	
	250,000	16.7	14.6	22.3	29.8	56.3	
	200,000	13.2	11.5	17.8	23.9		
90	150,000	6.4	8.9	13.4	17.9		
	100,000	4.3	5.8	10.1	11.8		
	50,000	2.3	3.1	4.6	6.3		
	250,000	10.8	15.1	22.8	31.1		
	200,000		10.0	18.3	24.5		
120	150,000		9.3	13.8	18.4		
	100,000		6.0	9.5	12.3		
	50,000		3.6	5.0	6.7		
	250,000			22.8	30.6		
	200,000			18.4	24.7		
150	150,000	Low Quality		14.1	18.3		
	100,000				12.6		
	50,000						
	250,000				31.8		
	200,000				25.5		
200	150,000				19.4		
	100,000				12.7		
	50,000						

VI. CONCLUSIONS

45

The local heat transfer coefficients are much higher in the boiling region than in the liquid region.

The local heat transfer coefficients increase with increasing quality up to a quality near 0.50, whereupon the coefficients decrease rapidly toward a gas film coefficient which is reached near a quality of 0.70 for these tests.

The measured local heat transfer coefficients can be presented in one equation involving dimensionless groups.

$$\frac{h\,D_e}{k} = \left[4.3 + 5.0 \times 10^4 \left(\frac{V_{fg}}{V_f}\right)^{1.64} \times\right]\left(\frac{q''}{Gh_{fg}}\right)^{0.464} \left(\frac{G\,D_e}{\mu_f}\right)^{0.808}$$

The equation can be used in the range of qualities from 0 to 40%.

The dimensionless groups appear to be significant parameters for use in correlating local boiling data of other investigators.

A more extensive investigation should be undertaken to include a greater variation of heat flux, flow and absolute pressure.

ACKNOWLEDGEMENT

The author wishes to express his gratitude for the assistance he has been given to make this work possible. Mr. A. S. Jameson, Head of the Engineering Section, was most generous with time and equipment, and showed a continued interest in the work. Mr. R. Rohde, also of Heat Engineering Section, was most helpful during the experimental and computational phases. The cooperation of Dr. J. C. Boyce of Argonne National Laboratory, where the work was carried out, is gratefully acknowledged.

The many helpful suggestions of Professor Max Jakob, the author's advisor, contributed greatly to the successful completion of the enterprise. Thanks are also expressed for the help given by Professor F. D. Carvin, Director of the Department of Mechanical Engineering, Illinois Institute of Technology.

50

APPENDIX A

TABULATION OF DATA

Table III is a compilation of the measured and calculated quantities for all of the runs used in the analysis. The first 60 runs were preliminary and were not used in the analysis. It was initially conceived to have local boiling conditions over a large fraction of the test section and the rest of the section in the region of net steam generation. Unfortunately, not enough of the section could be held in the local boiling region and still nave large enough exit qualities to adequately study the transition region. These runs were then used mainly to become acquainted with the operating characteristics of the apparatus.

51

Table III

EXPERIMENTAL DATA

Pressure - 45 psia				
Run No.	$G/10^6$ lb / (hr)(sq ft)	$q''/10^6$ Btu / (hr)(sq ft)	x, %	θ_{sat}, F
75	1.02	0.05	0	10.9
			0.5	10.4
			1.0	9.7
75		0.05	2.0	8.0
76		0.100	0	23.0
			1.0	18.4
			2.0	15.2
76		0.100	3.76	11.2
77		0.150	0	27.7
			1.0	24.4
			2.0	21.5
			4.0	16.4
77		0.150	5.8	13.9
78		0.200	0	31.2
			1.0	29.0
			3.0	23.0
			5.0	19.6
78		0.200	7.7	18.9
79		0.250	0	33.6
			1.0	31.5
			3.0	27.0
			6.0	23.0
79		0.250	9.4	23.0
74	0.765	0.765	0	13.1
			1.0	11.5
74	0.765		2.0	10.0
74	0.765	0.05	2.95	9.0
73		0.100	0	23.8
			1.0	21.0
			2.0	19.0
			4.0	15.0
73		0.100	5.46	12.8
72		0.151	0	29.4
			2.0	25.1
			4.0	20.2
			6.0	17.7
72		0.151	8.0	15.7
		0.200	0	33.7
71			3	28
			6	23.7
			9	20.5
71		0.200	10.7	19.7
70		0.250	0	31.1
			3	27.6
			6	24.6
			9	22.6
			12	22.6
70		0.250	13.2	22.6
63	0.51	0.100	0	23.8
			2.0	20.7
			4.0	18.8
			6.0	16.3
63		0.100	8.4	14.6

Pressure - 45 psia				
Run No.	$G/10^6$ lb / (hr)(sq ft)	$q''/10^6$ Btu / (hr)(sq ft)	x, %	θ_{sat}, F
62		0.150	0	31
			3.0	27.4
			6.0	23.7
			9.0	18.9
62		0.150	12.5	17.7
61		0.200	0	33.2
			4.0	28.3
			8.0	23.4
			12	20.5
61		0.200	17	18.5
60A		0.250	0	37.2
			4.0	32.0
			8.0	28.0
			12	24.3
			16	21.4
60A		0.250	20.6	20.0
69	0.382	0.05	0	15.6
			2.0	14.2
			4.0	12.4
69		0.05	5.8	11.6
68		0.100	0	29
			3.0	25
			6.0	21
			9.0	18
68		0.100	11.3	15.1
67		0.150	0	32.8
			4.0	28.3
			8.0	25.4
			12.0	22.3
			16.0	19.8
67		0.150	17.2	19.0
66A		0.200	0	36.9
			5.0	31.8
			10.0	27.7
			15.0	23.5
			20.0	20.7
66A		0.200	22.7	20.0
65B		0.250	0	42
			5.0	37.2
			10.0	33.0
			15.0	29.6
			20.0	26.5
			25.0	23.3
65B		0.250	28.4	22.5
139	0.255	0.05	0	17.9
			4.0	15.5
			88.0	11.9
139		0.05	11.2	10.1
138		0.100	0	32
			4.0	30.7
			8.0	22.7
			12.0	14.4
			16.0	14.3
138		0.100	21.4	13.5

52

Table III
(Cont'd)

Pressure - 45 psia

Run No.	G/10⁶ lb (hr)(sq ft)	q"/10⁶ Btu (hr)(sq ft)	x, %	θ_{sat}, F
137		0.150	0	41.5
			4.0	38.9
			8.0	31.9
			12.0	23.8
			15.0	20.9
			20.0	19.1
			24.0	17.2
			28.0	16.6
137		0.150	32.3	15.9
136	0.25	0.200	0	45
			5.0	41.5
			10.0	33.7
			15.0	26.7
			20.0	23.5
			25.0	21.5
			30.0	19.8
			35.0	19.5
			40.0	17.5
			41.0	17.2
			42.0	18.8
136		0.200	43.2	22.5
135		0.250	0	45.1
			5.0	41.8
			10.0	38.4
			15.0	35.1
			20.0	32.1
			25.0	28.8
			30.0	26.7
			35.0	24.9
			40.0	23.0
			45.0	20.8
			47.0	21.1
			48.0	21.6
			50.4	24.4
			52.0	27.9
135	0.255	0.250	54.4	33.5
	Pressure - 90 psia			
84	1.02	0.05	0	10.9
			1.0	9.9
			2.0	8.9
84		0.05	2.3	8.8
83		0.100	0	16.0
			1.0	14.8
			2.0	12.8
			3.0	11.8
83		0.100	4.3	11.4
82		0.150	0	20
			2.0	17.7
			4.0	16.7
82		0.150	6.4	16.5
81		0.200	0	22.7
			1.0	21.7
			3.0	20.0
			5.0	18.8
81		0.200	8.5	17.6

Pressure - 90 psia

Run No.	G/10⁶ lb (hr)(sq ft)	q"/10⁶ Btu (hr)(sq ft)	x, %	θ_{sat}, F
80		0.250	0	26
			1.0	25
			2.0	24.2
			4.0	22.8
			6.0	22.0
			8.0	22.0
80	1.02	0.250	10.8	22.1
85	0.765	0.05	0	11.4
			1.0	10.5
			2.0	10.2
85		0.05	3.1	10.4
86		0.100	0	118
			1.0	17
			2.0	16
			3.0	15.7
			4.0	14.6
86		0.100	5.8	13.6
87		0.150	0	23.5
			2.0	21.7
			4.0	18.7
			6.0	17.6
87		0.150	8.8	16.0
88		0.20	0	25.6
			3.0	22.7
			6.0	21.0
			9.0	20.0
88		0.20	11.5	18.8
89		0.25	0	25.3
			3	24.0
			6	22.6
			9	22.9
			12	23.1
89		0.25	14.6	22.9
90	0.51	0.05	0	12.6
			1.0	11.9
			2.0	11.4
			3.0	10.4
90		0.05	4.6	9.6
91		0.100	0	24.8
			2.0	22.5
			4.0	19.8
			5.0	17.2
			8.0	15.5
91		0.100	10.1	13.8
92		0.150	0	27.9
			3	26.0
			6	24.0
			9	21.7
92		0.150	13.4	19.1
93		0.20	0	29
		4.0	4.0	27.3
			8.0	24.9
			12.0	23.7
			16.0	22.7
93		0.20	17.8	22.7

Table III
(Cont'd)

Pressure - 90 psia

Run No.	G/10[6] lb (hr)(sq ft)	q"/10[6] Btu (hr)(sq ft)	x, %	θ_{sat}, F
94		0.25	0	32.9
			5.0	31.2
			10.0	29.1
			15.0	27.8
			20.0	26.3
94	0.51	0.25	22.3	25.8
99	0.382	0.050	0	14.4
			2.0	13.9
			4.0	13.4
99		0.05	5.3	12.9
98		0.100	0	22.2
			3.0	22.2
			6.0	20.2
			99.0	17.3
98		0.100	11.8	14.4
97		0.150	0	26.2
			4.0	25.0
			8.0	23.4
			12.0	22.3
97		0.150	17.9	21.0
96		0.20	0	29.0
			6.0	27.2
			12.0	25.7
			18.0	24.4
96		0.20	23.9	23.2
95		0.25	0	31.9
			6.0	30.6
			12.0	29.1
			18.0	28.6
			24.0	28.0
95	0.382	0.25	29.8	27.2
140	0.255	0.250	0	46.9
			3.0	44.9
			6.0	40.9
			9.0	34.4
			12.0	26.9
			15.0	21.1
			20.0	20.1
			30.0	20.0
			40.0	19.5
			50.0	19.5
			53.0	19.4
140	0.255	0.250	55.0	21.6
			56.3	24.6

Pressure - 120 psia

Run No.	G/10[6] lb (hr)(sq ft)	q"/10[6] Btu (hr)(sq ft)	x, %	θ_{sat}, F
100	1.02	0.250	0	24.2
			3	21.9
			5	20.6
			9	19.5
100	1.02	0.250	10.8	18.7
109	0.765	0.05	0	13.9
			1.0	12.9
			2.0	12.4
109			3.0	12.4
109		0.05	3.6	12.0
108		0.100	0	14.8
			2.0	14.0
			4.0	13.8
108		0.100	6.0	13.8
107		0.150	0	19.7
			2.0	18.7
			4.0	17.3
			6.0	16.2
			8.0	15.8
107		0.150	9.3	15.2
106		0.200	0	22.4
			2.0	21.2
			4.0	19.7
			6.0	18.4
			8.0	18.0
106		0.200	10.0	16.6
105		0.250	0	26.5
			4.0	23.0
			8.0	22.5
			12.0	21.5
105	0.765	0.250	15.1	20.5
110	0.51	0.05	0	13.1
			2.0	11.9
			4.0	10.9
110		0.05	5.0	10.6
111		0.100	0	20.3
			2.0	19.8
			4.0	18.8
			6.0	18.2
			8.0	18.0
111		0.100	9.5	17.2
112		0.150	0	23.1
			3.0	22.1
			6.0	20.9
			9.0	20.6
			12.0	19.5
112		0.150	13.8	19.2
113		0.200	0	26.6
			4.0	25.5
			8.0	24.7
			12.0	23.7
			16.0	23.2
113		0.200	18.3	22.7
114		0.250	0	30.1
			4.0	29.5
			8.0	28.5
			12.0	27.5
			16.0	26.6
			20.0	26.1
114	0.51	0.250	22.8	26.0
119	0.382	0.050	0	13.1
			2.0	12.6
			4.0	12.5
			6.0	12.4
119		0.050	6.7	12.4

Table III
(Cont'd)

Run No.	$G/10^6$ lb (hr)(sq ft)	$q''/10^6$ Btu (hr)(sq ft)	x, %	θ_{sat}, F
Pressure - 120 psia				
118		0.100	0	21.3
			3.0	20.5
			6.0	19.7
			9.0	18.8
118		0.100	12.3	17.8
117		0.150	0	25.1
			4.0	24.2
			8.0	23.3
			12.0	22.7
			16.0	22.4
117		0.150	18.4	21.7
116		0.200	0	28.9
			5.0	27.7
			10.0	27.3
			15.0	26.7
			20.0	25.7
116		0.200	24.5	25.6
115		0.250	0	31.2
			5.0	30.4
			10.0	29.5
			15.0	28.7
			20.0	28.5
			25.0	27.5
115	0.382	0.250	31.1	27.0
Pressure - 150 psia				
127	0.51	0.150	0	25.9
			3.0	23.8
			6.0	21.9
			9.0	19.5
			12.0	17.7
127		0.150	14.1	15.7
126		0.200	0	31.2
			3.0	28.9
			6.0	27.0
			9.0	25.1
			12.0	22.9
			15.0	20.7
126		0.200	18.4	19.0
125		0.250	0	28.6
			4.0	27.1
			8.0	25.6
			12.0	23.6
			16.0	22.1
			20.0	20.6
125	0.51	0.250	22.8	20.0
123	0.382	0.100	0	19.3
			3	18.3
			6	17.7
			9	17.5
123		0.100	12.6	16.2

Run No.	$G/10^6$ lb (hr)(sq ft)	$q''/10^6$ Btu (hr)(sq ft)	x, %	θ_{sat}, F
Pressure - 150 psia				
122		0.150	0	20.7
			3	20.2
			6	19.9
			9	19.9
			12	19.5
			15	19.3
122		0.150	18.3	19.3
121		0.200	0	26
			4	26
			8	25.7
			12	25.7
			16	25.1
			20	25.2
121		0.200	24.7	24.9
120		0.250	0	31.4
			5	30.4
			10	29.4
			15	28.6
			20	28.3
			25	27.6
120	0.382	0.250	30.6	26.8
133	0.382	0.100	0	22.3
			3.0	21.3
			6.0	20.5
			9.0	19.5
Pressure - 200 psia				
133		0.100	12.7	18.7
132		0.150	0	23.7
			4.0	22.9
			8.0	22.2
			12.0	21.2
			16.0	21.1
132		0.150	19.4	20.7
131		0.200	0	28.7
			5.0	27.9
			10.0	27.0
			15.0	26.1
			20.0	25.8
131		0.200	25.5	24.7
130		0.250	0	29.9
			5.0	30.1
			10.0	29.5
			15.0	29.6
			20.0	28.6
			25.0	28.3
130	0.382	0.250	31.8	28.3

APPENDIX B

ESTIMATE OF EXPERIMENTAL ERROR

Lineal Measurements

The test section was a seamless drawn tube, selected for conformance with dimensional specifications. The possible variation in wall thickness could account for less than 1% error in calculating the temperature drop through the wall.

Flow Rate

The flow rate, which was measured by means of calibrated orifices and U-tube manometer, was estimated to be in error by ± 1% maximum.

Temperature

All thermocouples were calibrated in place but not attached to the surface. The accuracy of the measurements was estimated at ± 1 F. The inlet and outlet thermocouples were calibrated in their final position; the accuracy was ± 0.5F.

Power

The electrical power measurement was subject to error in the wattmeter and in the instrument transformers. The wattmeter was calibrated before use and was found to have negligible error. With a pure resistance load, the instrument transformers had less than ± 0.25% error each because of phase shift. Power measurement then was probably accurate to ± 0.5%.

Pressure Measurements

The Bourdon-tube pressure gages used for experimental readings were precision-type and were calibrated. It was estimated that the pressure readings were correct to ± 1.0%.

Pressure drop was read on 60-inch well-type manometers with correlation for the change of interface level in the wall. The maximum error in these readings was estimated at ± 1.0 in. of water.

BIBLIOGRAPHY

1. Rohsenow, W. M., "Heat Transfer with Evaporation," Heat Transfer Symposium, University of Michigan, (1952) Section 4

2. Stroebe, G. W. et al, "Boiling - Film Heat Transfer Coefficients in a Long Tube Vertical Evaporator," Industrial and Engineering Chemistry, 31, 200 (1939)

3. Davidson, W. F., et al., "Studies of Heat Transmission Through Boiler Tubing at Pressures from 500 to 3300 Pounds," Transactions of the American Society of Mechanical Engineers, 65, 553 (1943)

4. McAdams, W. H., et al., "Vaporization Inside Horizontal Tubes," Transactions of the American Society of Mechanical Engineers, 63, 545 (1941)

5. Nukiyama, S., Journal of the Society of Mechanical Engineers, Japan, 37, 367 (1934), (English Abstract on p. 5 - 53)

6. Farber, E. A. and Scorah, R. L. "Heat Transfer to Boiling Water under Pressure," Transactions of the American Society of Mechanical Engineers, 70, 369 (1948)

7. Jakob, M., Heat Transfer, [New York: John Wiley and Sons (1949)], Vol. I, Chapter 29

8. Leppert, G., "Pressure Drop During Forced Circulation Boiling," Unpublished PhD Thesis, Illinois Institute of Technology (1953)

9. Grace, H. P. and Lapple, C. E., "Discharge Coefficients of Small Diameter Orifices and Flow Nozzles," Transactions of the American Society of Mechanical Engineers, 73, 639 (1951)

10. Wilson, E. E., "A Basis for Rational Design of Heat Transfer Apparatus," Transactions of the American Society of Mechanical Engineers, 37, 47 (1915)

11. Dittos, F. W., and Boelter, L. M. K., "Heat Transfer in Automobile Radiators of the Tubular Type," University of California Publications in Engineering, Vol. 2, No. 13, (1930), p. 443

12. Colburn, A. P., "A Method of Correlating Forced Convection Heat Transfer Data and A Comparison with Fluid Friction," Transactions of the American Institute of Chemical Engineers, 19, (1933)

13. Rohsenow, W. M., and Clark, J. A. "Heat Transfer and Pressure Drop Data for High Heat Flux Densities to Dates at High Sub-Critical Pressures," Heat Transfer and Fluid Mechanics Institute Stanford University Press, Stanford, California, (1951), p. 193

14. Buchberg, H., et al., "Final Report on Studies in Boiling Heat Transfer," University of California, Department of Engineering, Report COO-24, (1951)